Journal of Water Resource and Protection, 2025, 17(12), 866-901
https://www.scirp.org/journal/jwarp
ISSN Online: 1945-3108
ISSN Print: 1945-3094

# Assessing the Impact of Land Use and Land Cover Dynamics on Flood Risks in the Urban Areas of Abomey and Bohicon (Benin)

**Joachim Tobada[1], Peace Hounkpe[1,2], Guy Oyéniran Adeoti[1,2], Brice Gbaguidi[3]**

[1]School of Science, Technology, Engineering and Mathematics of Abomey, Abomey, Benin
[2]National University of Science, Technology, Engineering and Mathematics of Abomey, Abomey, Benin
[3]School of Engineering Sciences, University of Abomey-Calavi, Abomey-Calavi, Benin
Email: adeotiguy@unstim.bj

**How to cite this paper:** Tobada, J., Hounkpe, P., Adeoti, G.O. and Gbaguidi, B. (2025) Assessing the Impact of Land Use and Land Cover Dynamics on Flood Risks in the Urban Areas of Abomey and Bohicon (Benin). *Journal of Water Resource and Protection*, **17**, 866-901.
https://doi.org/10.4236/jwarp.2025.1712047

**Received:** October 13, 2025
**Accepted:** December 21, 2025
**Published:** December 24, 2025



## Abstract

Flooding is one of the most concerning natural hazards for urban populations in West Africa, particularly in the Beninese cities of Abomey and Bohicon. In these areas, vulnerability is exacerbated by the combined effects of recurring extreme rainfall events and unplanned urban expansion. This study aims to analyze land use and land cover (LULC) dynamics in both cities between 2005 and 2025, and to assess their impact on flood risk. The adopted methodology is based on the analysis of multispectral Landsat satellite imagery, which was pre-processed and subjected to supervised classification using the Maximum Likelihood method. Five land use categories were identified and compared across three reference years: 2005, 2015, and 2025. The results reveal a rapid expansion of built-up areas at the expense of vegetated and wetland zones, leading to increased surface imperviousness, a significant rise in runoff coefficients and flow velocities, and, consequently, heightened flood risks. These spatial dynamics underscore the urgent need for more resilient urban planning, incorporating land-use strategies tailored to sustainable stormwater management.

## Keywords

Flood Risk, Land Use/Land Cover (LULC), Urbanization, Landsat Imagery, West African Cities

## 1. Introduction

Rapid urbanization, combined with growing land pressure and the progressive

impermeabilization of soils, constitutes a major aggravating factor for urban flood risks due to stormwater runoff [1]. This urban sprawl increases vulnerability in two key ways: first, by encouraging the development of built-up areas in highly hazard-prone zones, and second, by rendering existing drainage infrastructure obsolete, as it is often undersized to cope with stormwater evacuation needs [2].

In many regions of the world—particularly in West Africa—uncontrolled urban expansion and land use changes contribute to amplifying the vulnerability of territories to extreme weather events [3] [4]. The cities of Abomey and Bohicon, located in the heart of Benin, are emblematic of this issue. Their geographic position, combined with current land-use dynamics, exposes them to recurring flood events with significant consequences for public health, the local economy, and the environment.

This study aims to analyze the impact of land use dynamics on flood risks in the cities of Abomey and Bohicon. It relies on a combined approach, integrating spatial analysis based on satellite imagery and field observations, to better understand the interactions between urban expansion and hydrological phenomena. The ultimate objective is to provide decision-making tools for territorial stakeholders in charge of urban planning and risk management.

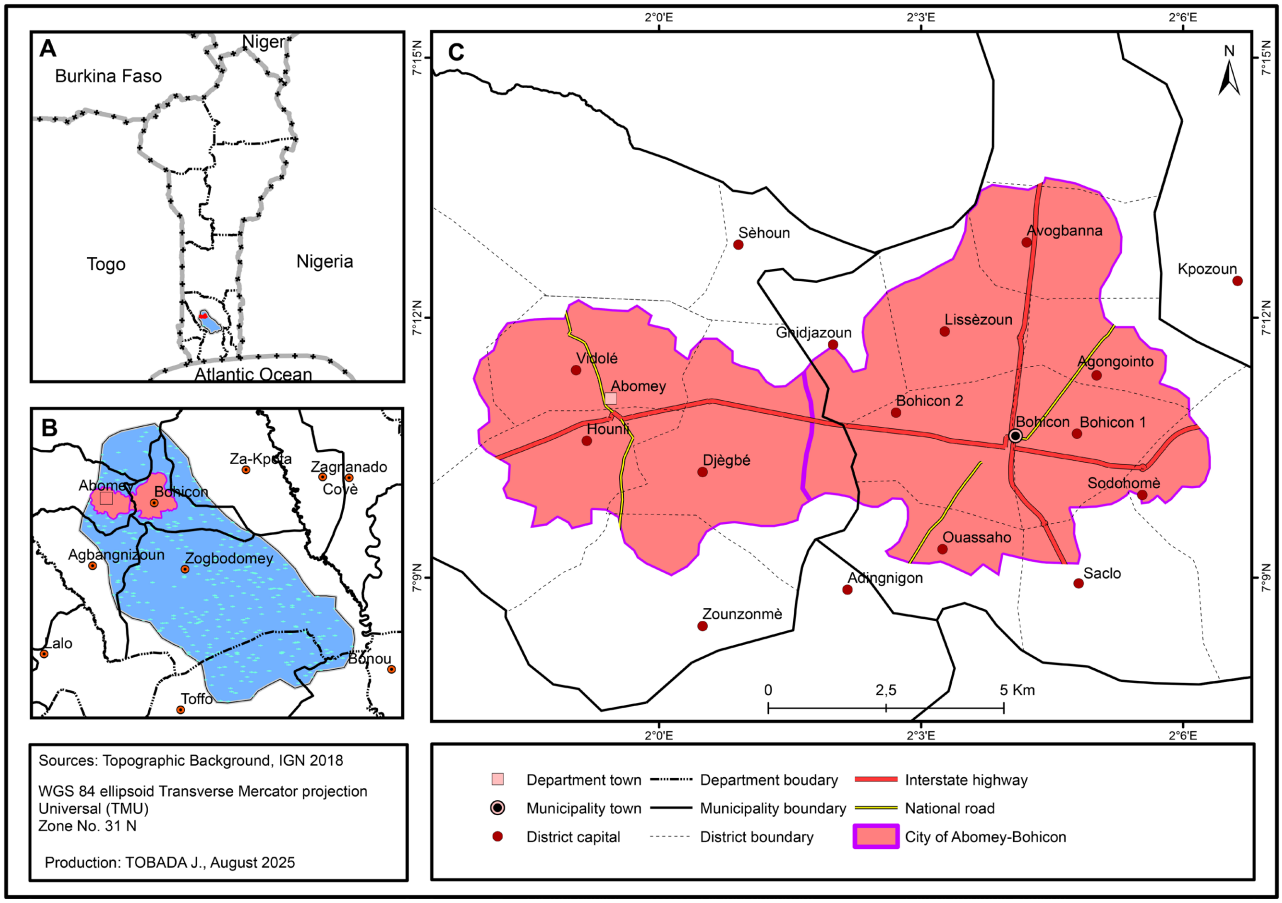


**Figure 1.** Geographical location map, administrative boundaries, and spatial extent of the cities of Abomey and Bohicon within the Hlan sub-watershed (Benin). Source: IGN Topographic Base Map, 2018. Map designed by: TOBADA J., December 2024.

### Study Area

The geographical scope of this research encompasses the cities of Abomey and Bohicon, located in southern Benin. These two urban centers lie within the Hlan sub-watershed, which is geographically delimited between longitudes 1˚54' and 2˚25' East, and latitudes 7˚10' and 7˚58' North. This watershed is bordered to the North and East by the Zou basin, to the west by the Couffo basin, and to the south by the Ouémé basin. It spans a total area of 1224 square kilometers.

Figure 1 illustrates the geographical location of the cities of Abomey and Bohicon, their administrative organization, as well as their spatial extent within the Hlan sub-watershed. This sub-watershed, with its 1224 km$^2$ area, forms a crucial hydrological entity that interfaces with three major surrounding basins: Zou, Couffo, and Ouémé.

## 2. Methodology

### 2.1. Planimetric Data and Satellite Image Sources

The spatio-temporal analysis of land use and land cover (LULC) was based on the exploitation of planimetric data and multi-source satellite imagery. The datasets used include:

- A 1:200,000 topographic map (sheet NC-31-XXI, Zou Department), produced by the French Geographic Institute [5], serves as a basis for geographic contextualization and validation of administrative boundaries;
- Satellite images from various missions: SPOT 6 (2005), SPOT 7 (2015), and Sentinel-2A (2024), cover the same scene (Path 192/Row 053) with different spatial resolutions.

The images used have medium spatial resolution (6 m for SPOT, 10 m for Sentinel-2, and 30 m for Landsat images used as secondary support), and were projected in the UTM Zone 31 North coordinate system using the WGS84 ellipsoid. These images were downloaded from the USGS Earth Explorer platform in GeoTIFF format, including precise geodetic metadata. Due to the prior correction for georeferencing and radiometric distortion (level L1T), no additional geometric rectification was required.

The technical characteristics of the satellite scenes used are summarized in Table 1 below:

Table 1. Technical specifications of satellite images used in the study.

| Satellite | Path/Row | Spatial Resolution | Scenes Used | Acquisition Date |
|---|---|---|---|---|
| SPOT 6 | – | 6 m | P191R53/P192R53 | December 25, 2005 |
| SPOT 7 | – | 6 m | P191R53/P192R53 | January 15, 2015 |
| Sentinel-2A | 192/055 | 10 m | P191R53/P192R53 | January 25, 2024 |

## 2.2. Tools and Equipment Used

The methodology relied on a combination of software tools, field equipment, and data processing resources, including:

- **Idrisi Selva 17.0**: used for supervised classification and satellite image processing;
- **ArcGIS 10.4**: used for thematic mapping, vectorization, and spatial analysis;
- **High-precision GPS**: for field surveys and ground-truth validation of control points;
- **Excel**: for structuring and processing statistical data derived from the classification.

## 2.3. Digital Processing and Land Use Classification

The methodological approach to satellite image analysis involved the following steps:

### 2.3.1. False Color Composite Generation

False color composites were generated by combining different spectral bands to enhance visual differentiation of land cover features (e.g., vegetation, built-up areas, bare soil). These combinations leverage the unique spectral signatures of each feature type. The common band combinations used include:

- Red-Near Infrared-Green (R-NIR-G) for SPOT imagery;
- Bands 4-3-2 and 8-4-3 are for Sentinel-2 imagery.

### 2.3.2. Delineation of Training Areas

Training areas are homogeneous zones selected on the images to represent each land use class (built-up areas, dense vegetation, cropland, bare soil, wetlands, etc.). These zones must:

- Be located away from ecotones to avoid mixed pixels;
- Be sufficiently numerous and well-distributed across the scene;
- Have appropriate sizes: larger than the localization error but smaller than the average size of the objects being mapped [6].

The quality of the classification highly depends on the representativeness and homogeneity of these training areas.

### 2.3.3. Supervised Classification Using Maximum Likelihood

The Maximum Likelihood Classification (MLC) method was chosen due to its ability to consider intra-class variance and covariance. The algorithm computes the probability of each pixel belonging to a given class based on its statistical distance from the spectral means of the classes.

Each pixel is then assigned to the class for which it has the highest likelihood, resulting in an optimized and statistically robust classification output.

### 2.3.4. GIS Validation and Export

After classification, the results were exported in raster format to ArcGIS, then converted into vector format (shapefiles) for further quantitative analysis. The

surface area of each land use class was calculated using spatial analysis tools and compared over time to assess land use change dynamics. Field verification (using GPS) was conducted on a sample of points to validate the classification results.

## 2.4. Statistical Analysis of Land Use Dynamics

The evaluation of the spatio-temporal evolution of landscape units is based on a post-classification approach, which involves comparing land use maps generated for the periods 2005-2015 and 2015-2024. This analysis allows for the quantification of land use conversions, the measurement of their intensity, and the identification of dominant transformation trends [7].

### Transition Matrix of Landscape Units

The transition matrix is the central tool for analyzing landscape dynamics. It results from the overlay of land use maps at two different time points and provides insights into land cover conversions during the studied period.

Each matrix is generated using the "Intersect" function from the ArcToolbox of the ArcGIS 10.6 software [8]. Rows represent land use classes at the initial date ($t_1$), while columns correspond to classes at the final date ($t_2$). The main diagonal indicates stable land use areas, while off-diagonal values represent interclass conversions.

This method is particularly recommended for land use change studies, as it offers a precise analysis of transition flows between spatial units [9].

## 2.5. Conversion Rate of Landscape Units

The conversion rate measures the proportion of a landscape unit that has changed between two dates. It is useful for assessing a class's vulnerability to land pressure or anthropogenic dynamics [10] [11].

Formula:

$$T_C = \left( \frac{S_{it} - S_{is}}{S_{it}} \right) \times 100$$

where:

- $S_{it}$: Area of landscape unit $i$ at the initial date $t$.
- $S_{is}$: Area of the same unit that remained stable at date $t_1$.

This metric is widely used in landscape change studies [7].

## 2.6. Annual Average Spatial Expansion Rate

This rate assesses the relative pace of change of a land use class on an annual basis. It is useful for comparing the speed of expansion or regression among different units [10].

Formula:

$$T = \left( \frac{S_2 - S_1}{(t_2 - St_1) \times S_1} \right) \times 100$$

where:

- $S_1$, $S_2$: Area of the class at dates $t_1$ and $t_2$, respectively;
- $t_2 - t_1$: Time interval in years.

Already applied by [6] to assess land-use changes in East Africa, this indicator is also relevant in rapidly changing urban tropical contexts.

## 2.7. Rate of Land Use Evolution

The evolution rate expresses the absolute change in a land use class in hectares per year.

Formula:

$$\Delta S = \frac{SP_2 - SP_1}{t_2 - t_1}$$

where:

- $SP_1$ and $SP_2$: areas at dates $t_1$ and $t_2$, respectively.
- $\Delta S$: variation speed in hectares per year (ha/year).

This indicator complements relative rates by providing an absolute reading of land dynamics [12] [13].

## 2.8. Change Intensity Analysis

To better understand the structure of the observed transitions, an intensity analysis was performed using tools developed by [14]:

- PontiusMatrix22 (open-source software).
- IntensityAnalysis02.xlsm (Excel macro).

### 2.8.1. PontiusMatrix22

This tool generates graphs illustrating the transition intensities for each land use category and time interval. It distinguishes between:

- Dormant changes (below the uniform change line).
- Active changes (above this line).

This dynamic visualization, widely used in land change studies [9] [15], enables a qualitative assessment of the speed and intensity of land transformations.

### 2.8.2. IntensityAnalysis02.xlsm

This Excel workbook allows users to:

- Quantify net gains and losses by land unit.
- Analyze cross-class transitions.
- Visualize global and category-specific intensities of land use changes.

## 2.9. Evaluation of Classification Accuracy

The assessment of the classification quality was carried out using the confusion matrix, which compares classified pixels with reference data (ground truth). Several statistical indices were computed to quantify the performance of the classification, including the Class Purity Index (CPI), the Map Validity Index (MVI), the Omission Error (OE), the Commission Error (CE), and the Overall Accuracy Index (OAI).

#### 2.9.1. Class Purity Index (CPI)

The class purity index, also called producer's accuracy, measures the proportion of reference pixels from class $i$ that are correctly classified in that same class. It reflects the internal homogeneity of each mapped unit.

$$\text{CPI} = \frac{n_{ii}}{\sum_{j=1}^{n} n_{ij}} \times 100$$

$n_{ii}$ : Number of correctly classified pixels for class $i$ (values on the main diagonal).

$\sum_{j=1}^{n} n_{ij}$ : Total number of pixels of class $i$ in the reference data.

#### 2.9.2. Map Validity Index (MVI)

The map validity index, also referred to as user's accuracy, indicates the proportion of pixels assigned to a given class $i$ in the classification that are actually correct. It evaluates the reliability of the map for an end user.

$$\text{MVI} = \frac{n_{ii}}{\sum_{j=1}^{n} n_{ji}} \times 100$$

$n_{ii}$ : Number of correctly classified pixels for class $i$.

$\sum_{j=1}^{n} n_{ji}$ : Total number of pixels assigned to class $i$ in the classification.

#### 2.9.3. Omission Error (OE)

The omission error corresponds to the proportion of pixels that truly belong to class $i$ but were misclassified into other categories. It is complementary to the CPI.

$$\text{OE}_i = 100 - \text{CPI}_i$$

#### 2.9.4. Commission Error (CE)

The commission error represents the proportion of pixels assigned to class $i$ in the classification that do not actually belong to it (misclassified pixels). It is complementary to the MVI.

$$\text{EC}_i = 100 - \text{MVI}_i$$

#### 2.9.5. Overall Accuracy Index (OAI)

The overall accuracy index measures the proportion of correctly classified pixels in the entire confusion matrix.

$$\text{OAI} = \frac{\sum_{i=1}^{n} n_{ii}}{N} \times 100$$

$\sum_{i=1}^{n} n_{ii}$ Sum of correctly classified pixels (main diagonal).

*N*: total number of validation pixels used (sum of all elements in the matrix).

## 3. Results and Discussion

The analysis of spatio-temporal land use dynamics in the cities of Abomey and Bohicon is based on the interpretation of thematic maps derived from supervised classification, coupled with quantitative tools such as transition matrices, compar-

ative area graphs, and spatial evolution indicators. The 2005-2015 period reveals early significant territorial transformations linked to demographic pressure, urban expansion, and agricultural shifts.

### 3.1. Evaluation of the Interpretation of the 2005, 2015, and 2024 Images

The evaluation of the satellite image interpretation aims to measure the reliability and validity of the land-use/land-cover classifications derived from the Landsat images of 2005, 2015, and 2024. It is based on a comparison between the produced maps and reference data (field surveys, historical maps, high-resolution imagery). The classification quality is assessed using statistical indicators such as omission error (OE), commission error (CE), the Class Purity Index (CPI), the Map Validity Index (MVI), and the Overall Accuracy Index (OAI). The combined analysis of these parameters provides an objective assessment of the accuracy and consistency of the resulting maps, thereby ensuring the reliability of the outputs for the study of the spatio-temporal dynamics of landscape units.

#### 3.1.1. Accuracy and Validation of the 2005 Classification

Table 2 presents the confusion matrix of the 2005 SPOT-6 images.

Table 2. Confusion matrix and validation indices for the classification of the 2005 SPOT-6 images.

| Observed units | Interpretation | | | | | | | | | | | |
|---|---|---|---|---|---|---|---|---|---|---|---|---|
| | FCSB | SASa | FM | CJ | CJP | PLT | SN | PE | Ha | Total | IPC | EC |
| FCSB | 398 | 15 | 4 | 0 | 0 | 7 | 0 | 0 | 12 | 436 | 91.28 | 8.72 |
| SASa | 12 | 213 | 0 | 0 | 4 | 0 | 0 | 0 | 3 | 232 | 91.81 | 8.19 |
| FM | 0 | 5 | 124 | 0 | 0 | 0 | 0 | 8 | 0 | 137 | 90.51 | 9.49 |
| CJ | 0 | 12 | 0 | 185 | 12 | 0 | 0 | 0 | 0 | 209 | 88.52 | 11.48 |
| CJP | 0 | 0 | 0 | 11 | 198 | 9 | 5 | 0 | 1 | 224 | 88.39 | 11.61 |
| PLT | 10 | 0 | 0 | 0 | 5 | 133 | 0 | 0 | 0 | 148 | 89.86 | 10.14 |
| SN | 0 | 0 | 0 | 0 | 4 | 0 | 97 | 2 | 5 | 108 | 89.81 | 10.19 |
| PE | 1 | 0 | 0 | 0 | 0 | 0 | 0 | 68 | 0 | 69 | 98.55 | 1.45 |
| Ha | 0 | 0 | 0 | 3 | 2 | 0 | 5 | 0 | 95 | 105 | 90.48 | 9.52 |
| Total | 421 | 245 | 128 | 199 | 225 | 149 | 107 | 78 | 116 | 1668 | 91,02 | |
| IVC | 94.54 | 86.94 | 96.88 | 92.96 | 88.00 | 89.26 | 90.65 | 87.18 | 81.90 | 89.81 | | |
| EO | 5.46 | 13.06 | 3.13 | 7.04 | 12.00 | 10.74 | 9.35 | 12.82 | 18.10 | | | |
| **Overall accuracy** | | | | | **89.81** | | | | | | | |

FCSB refers to Open Forest and Wooded Savanna, SASa to Tree and Shrub Savanna, FM to Marsh Formation, CJ to Croplands and Fallows, CJP to Croplands and Fallows under Oil-Palm, PLT to Plantation, SN to Bare Soil, PE to Water Body, and Ha to Settlement. The accuracy indicators include OE (Omission Error), CE (Commission Error), CPI (Class Purity Index), MVI (Map Validity Index), and OAI (Overall Accuracy Index).

The classification of the 2005 SPOT-6 image shows good cartographic quality, with an overall accuracy of 89.81% and an average Class Purity Index (CPI) above 91%. The main confusions occur between open forests and wooded savannas (FCSB), tree- and shrub-dominated savannas (SASa), and the mosaic of croplands and fallows (CJ and CJP), with commission errors ranging from 8% to 12%. These confusions are largely due to the similarity of spectral signatures among vegetation covers and the presence of isolated trees within fallow areas. Marsh formations (FM) and plantations (PLT) exhibit good accuracy, with purity indices exceeding 89%, while water bodies (PE) are the best-classified unit, with only 1.45% omission and commission error. Conversely, the habitation class (Ha) records a relatively high omission error (18.10%), reflecting confusions with bare soils and newly established plantations. Overall, the accuracy achieved confirms the reliability and spatial consistency of the 2005 Landsat classification, which provides a solid foundation for analyzing the spatio-temporal dynamics of land use.

### 3.1.2. Accuracy and Validation of the 2015 Classification

Table 3 presents the confusion matrix of the 2015 SPOT-7 images.

Table 3. Confusion matrix and validation indices for the classification of the 2015 SPOT-7 images.

| Observed units | Interpretation | | | | | | | | | | | |
|---|---|---|---|---|---|---|---|---|---|---|---|---|
| | FCSB | SASa | FM | CJ | CJP | PLT | SN | PE | Ha | Total | IPC | EC |
| FCSB | 155 | 4 | 0 | 0 | 7 | 0 | 12 | 0 | 0 | 178 | 87.08 | 12.92 |
| SASa | 2 | 189 | 8 | 3 | 8 | 0 | 0 | 0 | 0 | 210 | 90.00 | 10.00 |
| FM | 0 | 1 | 75 | 3 | 0 | 0 | 0 | 2 | 1 | 82 | 91.46 | 8.54 |
| CJ | 0 | 0 | 6 | 123 | 4 | 0 | 2 | 0 | 0 | 135 | 91.11 | 8.89 |
| CJP | 10 | 0 | 5 | 6 | 133 | 0 | 0 | 0 | 0 | 154 | 86.36 | 13.64 |
| PLT | 0 | 0 | 0 | 8 | 0 | 168 | 0 | 8 | 0 | 184 | 91.30 | 8.70 |
| SN | 18 | 0 | 0 | 0 | 0 | 0 | 438 | 0 | 0 | 456 | 96.05 | 3.95 |
| PE | 0 | 0 | 0 | 2 | 0 | 7 | 0 | 184 | 0 | 193 | 95.34 | 4.66 |
| Ha | 0 | 0 | 0 | 0 | 0 | 0 | 3 | 0 | 65 | 68 | 95.59 | 4.41 |
| Total | 185 | 194 | 94 | 145 | 152 | 175 | 455 | 194 | 66 | 1660 | 91.59 | 88.86 |
| IVC | 83.78 | 97.42 | 79.79 | 84.83 | 87.50 | 96.00 | 96.26 | 94.85 | 98.48 | 90.05 | | |
| EO | 16.22 | 2.58 | 20.21 | 15.17 | 12.50 | 4.00 | 3.74 | 5.15 | 1.52 | | | |
| **Overall accuracy** | **90.05** | | | | | | | | | | | |

FCSB refers to Open Forest and Wooded Savanna, SASa to Tree and Shrub Savanna, FM to Marsh Formation, CJ to Croplands and Fallows, CJP to Croplands and Fallows under Oil-Palm, PLT to Plantation, SN to Bare Soil, PE to Water Body, and Ha to Settlement. The accuracy indicators include OE (Omission Error), CE (Commission Error), CPI (Class Purity Index), MVI (Map Validity Index), and OAI (Overall Accuracy Index).

The classification of the 2015 SPOT-7 image shows excellent cartographic quality, with an overall accuracy of 90.05% and an average Class Purity Index (CPI) of about 91.6%, indicating a strong correspondence between the classification and field observations. The highest performances are obtained for bare soils (SN), habitations (Ha), and water bodies (PE), whose omission and commission errors are below 5%, reflecting high spectral homogeneity and clear discrimination of these classes. However, some confusions persist between open forests and wooded savannas (FCSB), tree-shrub savannas (SASa), and croplands/fallows under oil-palm (CJP), with commission errors ranging from 10% to 13%. These errors are explained by the spectral similarity between tree vegetation and herbaceous fallows that include scattered woody species. Marsh formations (FM) and croplands/fallows (CJ) also show good accuracy, with purity indices above 90%, although some spectral mixing remains with neighbouring wetland and agricultural zones. Overall, the high values of CPI (>86%), MVI (≈90%), and the total accuracy above 90% confirm the reliability and spatial consistency of the 2015 Landsat classification, which constitutes a solid basis for analysing land-use dynamics between 2005 and 2024.

### 3.2. Accuracy and Validation of the 2024 Classification

Table 4 presents the confusion matrix of the 2024 Sentinel images.

**Table 4.** Confusion matrix and validation indices for the classification of the 2024 Sentinel images.

| Observed units | Interpretation | | | | | | | | | | | |
|---|---|---|---|---|---|---|---|---|---|---|---|---|
| | FCSB | SASa | FM | CJ | CJP | PLT | SN | PE | Ha | Total | IPC | EC |
| FCSB | 88 | 3 | 0 | 0 | 3 | 0 | 0 | 0 | 0 | 94 | 93.62 | 6.38 |
| SASa | 2 | 99 | 0 | 0 | 4 | 0 | 0 | 0 | 3 | 108 | 91.67 | 8.33 |
| FM | 0 | 0 | 76 | 3 | 0 | 0 | 0 | 2 | 0 | 81 | 93.83 | 6.17 |
| CJ | 0 | 0 | 4 | 180 | 6 | 4 | 0 | 0 | 3 | 197 | 91.37 | 8.63 |
| CJP | 0 | 5 | 1 | 0 | 93 | 0 | 0 | 0 | 0 | 99 | 93.94 | 6.06 |
| PLT | 0 | 0 | 0 | 4 | 0 | 78 | 0 | 0 | 1 | 83 | 93.98 | 6.02 |
| SN | 8 | 0 | 0 | 0 | 0 | 0 | 65 | 0 | 2 | 75 | 86.67 | 13.33 |
| PE | 0 | 0 | 0 | 0 | 0 | 2 | 0 | 166 | 0 | 168 | 98.81 | 1.19 |
| Ha | 0 | 0 | 0 | 2 | 0 | 0 | 5 | 0 | 55 | 62 | 88.71 | 11.29 |
| Total | 98 | 107 | 81 | 189 | 106 | 84 | 70 | 168 | 64 | 967 | **92.98** | |
| IVC | 89.80 | 92.52 | 93.83 | 95.24 | 87.74 | 92.86 | 92.86 | 98.81 | 85.94 | **92.18** | | |
| EO | 10.20 | 7.48 | 6.17 | 4.76 | 12.26 | 7.14 | 7.14 | 1.19 | 14.06 | | | |
| **Overall accuracy** | **92.18** | | | | | | | | | | | |

FCSB refers to Open Forest and Wooded Savanna, SASa to Tree and Shrub Savanna, FM to Marsh Formation, CJ to Croplands and Fallows, CJP to Croplands and Fallows under Oil-Palm, PLT to Plantation, SN to Bare Soil, PE to Water Body, and Ha to Settlement. The accuracy indicators include OE (Omission Error), CE (Commission Error), CPI (Class Purity Index), MVI (Map Validity Index), and OAI (Overall Accuracy Index).

The classification of the 2024 Sentinel image demonstrates excellent cartographic quality, with an overall accuracy of 92.18% and an average Class Purity Index (CPI) of 92.98%, showing a very strong correspondence between the classification and actual field conditions. The best performances are recorded for water bodies (PE), marsh formations (FM), open forests and wooded savannas (FCSB), and croplands/fallows under oil palm (CJP), with omission and commission errors below 7%. These results are explained by the good spectral distinction of these units, enhanced by the high radiometric resolution of the Sentinel sensors and the homogeneity of the observed surfaces. Croplands/fallows (CJ) and plantations (PLT) also display good classification quality, with purity indices above 91% and commission errors below 9%. However, some confusion remains between bare soils (SN) and habitations (Ha), which share similar spectral properties in densely urbanized areas, resulting in omission errors of 7.14% and 14.06%, respectively. Despite these slight inaccuracies, the high CPI values (>88%), the strong cartographic validity (MVI ≈ 92%), and the overall accuracy above 92% confirm the reliability, spatial coherence, and thematic precision of the 2024 Landsat classification. It thus provides a robust reference for detailed analysis of recent land-use dynamics and urban expansion from 2015 to 2024.

## 3.3. Landscape Dynamics between 2005 and 2015

### 3.3.1. Cartographic Interpretation

Figure 2 and Figure 3 illustrate the spatial distribution of land use units in 2005 and 2015, respectively. These maps highlight the following patterns:

- A growing concentration of residential areas in the urban poles of Abomey, Bohicon, Djègbé, and Ouassaho;
- A visible decline in temporary agricultural zones (fallow and cultivated lands), now fragmented or encroached upon by settlements;
- Peripheral expansion of built-up areas along major road axes (RNIE 2 and RNIE 4), reflects a linear and scattered urbanization;
- A slight increase in palm grove areas, especially in the southeast of Bohicon, was observed.

This spatial evolution is typical of transitional urban zones, where urban growth occurs mainly at the expense of cultivated land.

### 3.3.2. Graphical Analysis of Surface Changes

Figure 4 presents a comparative graph of the land area occupied by each landscape unit in 2005 and 2015. Key observations include:

- A notable decline in the surface area of fields and fallows (CJ), decreasing from approximately 2518 ha to 2013 ha, a loss of 505 ha;
- A net increase in residential areas (Ha) from 3744 ha to 3968 ha, a gain of 224 ha;
- An increase in palm grove cultivation areas (CJP) from 712 ha to 901 ha, a gain of 189 ha;
- A slight rise in plantations (PLT), indicates localized agricultural diversification.

The transformation is largely dominated by the conversion of temporary agri-

cultural lands, raising concerns about food security and the sustainable management of land resources.

### 3.3.3. Interpretation of the Transition Matrix (Table 5)

The transition matrix compares land use classes between 2005 (rows) and 2015 (columns). It allows for:

- Identification of stable classes (values along the diagonal).
- Quantification of conversion flows between units.
- Evaluation of net losses and gains.

Key highlights include:

- CJ → Ha: 180.63 ha of cultivated land were urbanized;
- CJP → Ha: 14 ha were converted into residential areas;
- SASa → Ha: 23 ha of savanna transformed into built-up areas;
- CJ → CJP: 355 ha converted into perennial crops;
- FM → CJ/CJP: 5 ha reclaimed for agriculture, indicating pressure on wetland zones.

Overall, urban settlements expanded primarily at the expense of CJ, CJP, and SASa classes, while cultivated lands were fragmented and partly converted to perennial plantations.

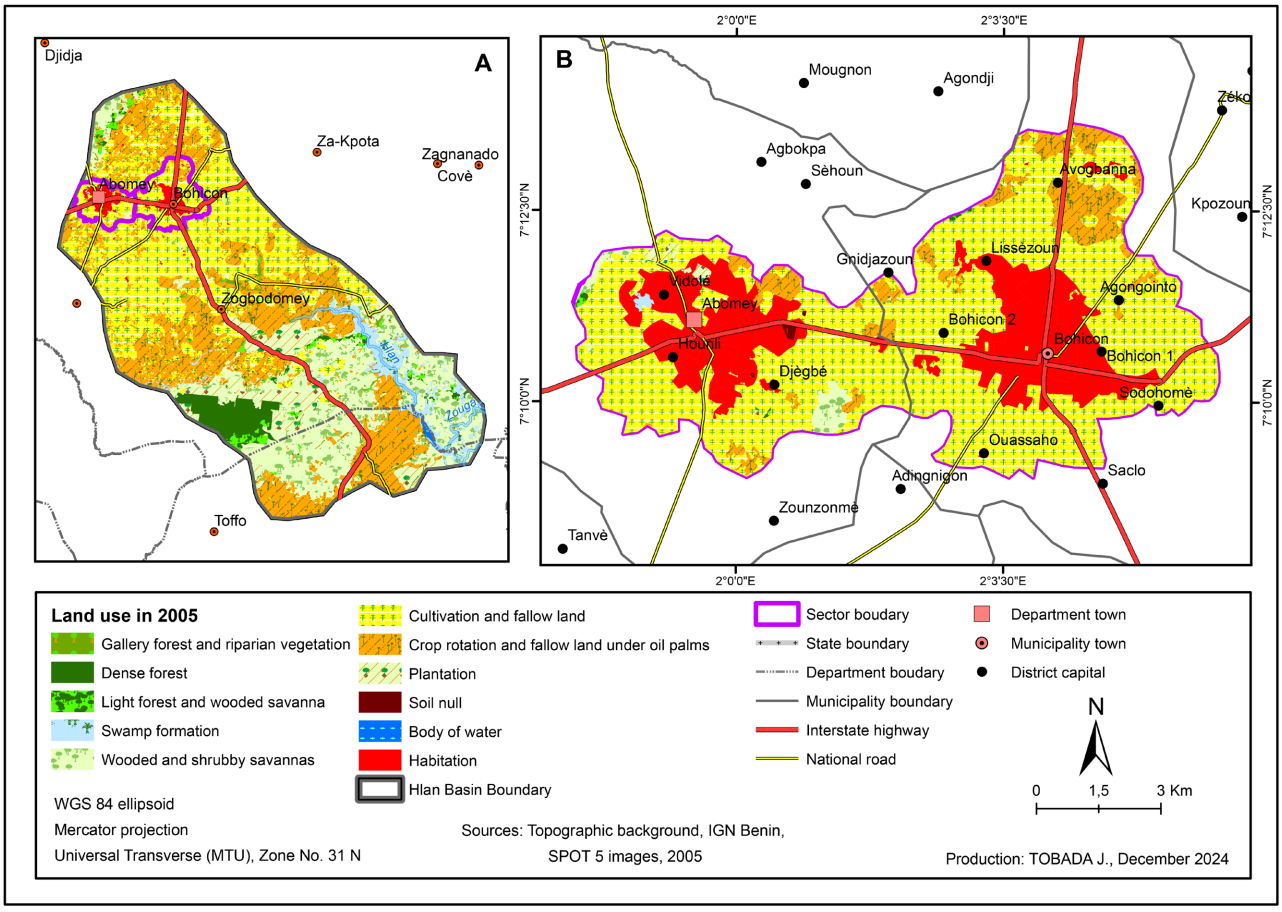


**Figure 2.** Land use map in 2005.

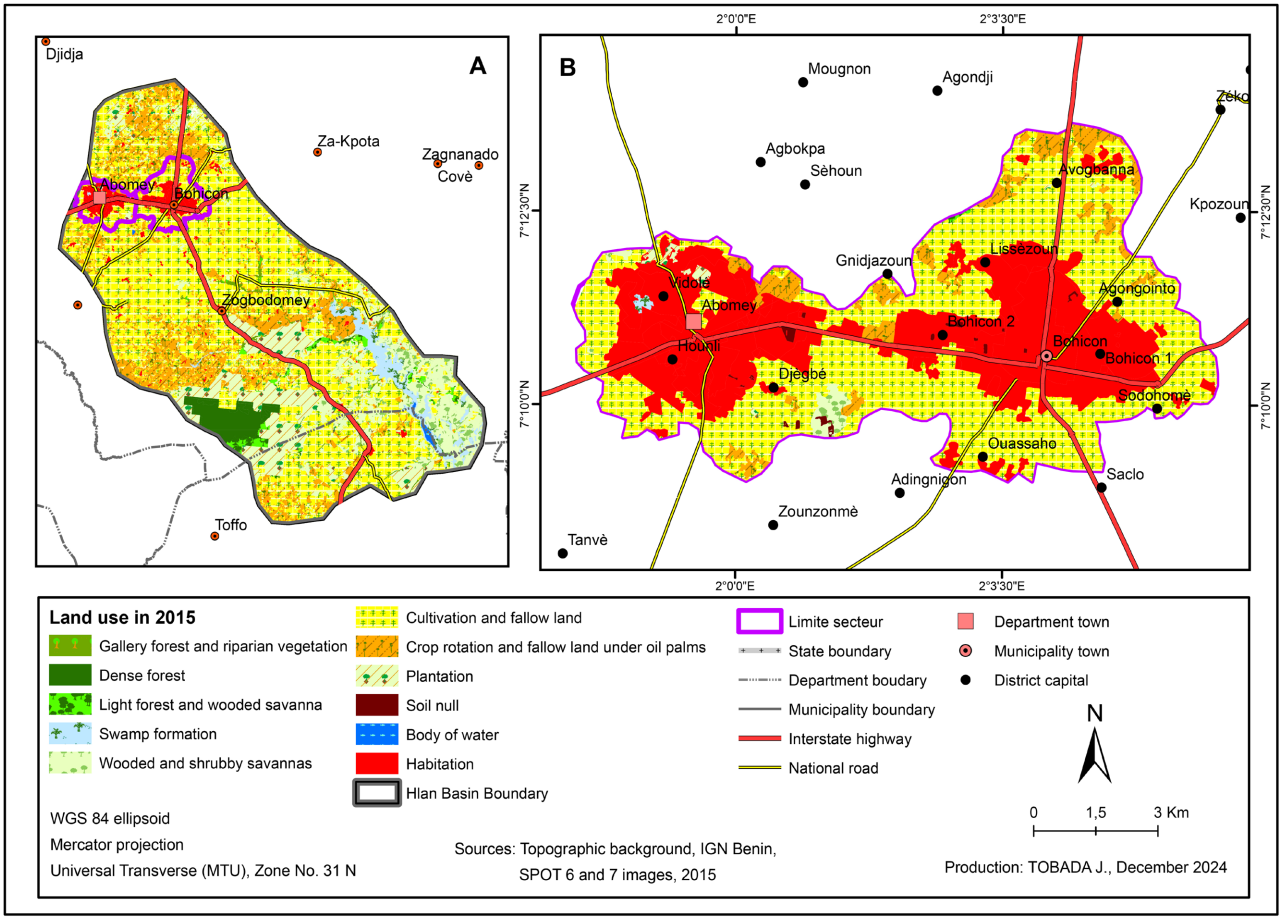


**Figure 3.** Land use map in 2015.

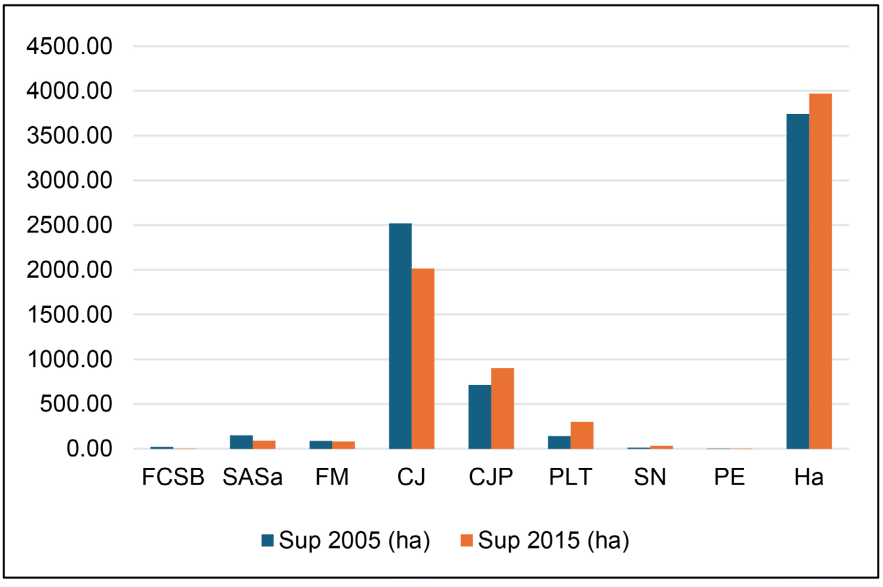


**Figure 4.** Change in land cover areas by class (2005-2015). FCSB: Open Forest-Wooded Savanna, SASa: Tree-Shrub Savanna, FM: Marshland Formation, CJ: Fields and Fallow, CJP: Fields and Fallow under Palm Plantations, PLT: Plantation, SN: Bare Soil, PE: Water Body, Ha: Settlement.

Figure 2 and Figure 3 respectively illustrate the land-use mapping of the study area in 2005 and 2015. These maps provide a visual overview of the spatial evolution of landscape units over the study period. A significant expansion of urban areas (in red) can be observed around the main road networks, along with a reduction in agricultural land (in yellow and orange), reflecting increasing anthropogenic pressure on the landscape.

Figure 4 shows the evolution of land-use units between 2005 and 2015, expressed in hectares. It highlights the changes in area for each land-use category, particularly the increase in residential zones and the decrease in agricultural land.

Table 5 presents this transition matrix, expressed in hectares, which allows the identification of the gains, losses, and conversions among the different landscape units.

**Table 5.** Land use transition Matrix between 2005 and 2015.

| Land Use Units (2005) | Land Use Units (2015) | | | | | | | | | | |
|---|---|---|---|---|---|---|---|---|---|---|---|
| | **FCSB** | **SASa** | **FM** | **CJ** | **CJP** | **PLT** | **SN** | **PE** | **Ha** | **Total 2005 (ha)** | Loss |
| **FCSB** | 3.00 | 2.00 | 0.00 | 10.00 | 3.00 | 3.00 | 0.00 | 0.00 | 1.00 | **22.00** | 19.00 |
| **SASa** | 0.00 | 88.63 | 0.00 | 17.35 | 8.00 | 7.00 | 8.00 | 0.00 | 23.00 | **151.98** | 63.35 |
| FM | 0.00 | 0.00 | 83.00 | 2.00 | 3.00 | 1.00 | 0.00 | 0.50 | 0.00 | **89.50** | 6.50 |
| CJ | 0.00 | 0.00 | 0.00 | 1823.00 | 355.00 | 148.63 | 11.00 | 0.00 | 180.63 | **2518.26** | 695.26 |
| **CJP** | 0.00 | 0.00 | 0.00 | 161.00 | 531.77 | 5.00 | 0.00 | 0.00 | 14.00 | **711.77** | 180.00 |
| **PLT** | 0.00 | 0.00 | 0.00 | 0.00 | 0.00 | 136.25 | 0.00 | 0.00 | 5.00 | **141.25** | 5.00 |
| **SN** | 0.00 | 0.00 | 0.00 | 0.00 | 0.00 | 0.00 | 12.04 | 0.00 | 0.00 | **12.04** | 0.00 |
| **PE** | 0.00 | 0.00 | 1.00 | 0.00 | 0.00 | 0.00 | 0.00 | 3.00 | 0.00 | **4.00** | 1.00 |
| **Ha** | 0.00 | 0.00 | 0.00 | 0.00 | 0.00 | 0.00 | 0.00 | 0.00 | 3744.66 | **3744.66** | 0.00 |
| **Total 2015 (ha)** | **3.00** | **90.63** | **84.00** | **2013.35** | **900.77** | **300.88** | **31.04** | **3.50** | **3968.30** | **7395.46** | **970.11** |
| **Gain** | 0.00 | 2.00 | 1.00 | 190.35 | 369.00 | 164.63 | 19.00 | 0.50 | 223.63 | **970.11** | |

Legend: FCSB: Open Forest-Wooded Savanna; SASa: Tree-Shrub Savanna; FM: Marshland Formation; CJ: Fields and Fallow; CJP: Fields and Fallow under Palm Groves; PLT: Plantation; SN: Bare Soil; PE: Water Body; Ha: Settlements.

### Interpretation (2005-2015)

The 2005-2015 period is characterized by progressive and steady urbanization, marked by both direct and indirect conversion of agricultural and natural lands into residential areas. This trend highlights:

- High land pressure, particularly along major transportation corridors.

- A decline in food-producing lands, potentially threatening urban food security.
- Increased surface runoff due to the gradual impermeabilization of soils.

The observed dynamics reflect a gradual substitution of temporary agricultural lands by urban settlements, a common pattern in rapidly expanding urban areas. This phenomenon is further exacerbated by the absence of adequate land-use planning.

The expansion of palm groves may be interpreted as:

- A shift toward cash crop production, or
- An indication of agricultural intensification on smaller land parcels.

Conversely, the loss of fallow and open areas poses ecological challenges regarding biodiversity conservation, water retention capacity, and environmental resilience.

### 3.4. Landscape Dynamics between 2015 and 2024

The diachronic analysis of land use between 2015 and 2024 reveals strong patterns of landscape transformation. Based on remote sensing data and post-classification comparison, the overall trend shows increasing urbanization at the expense of agricultural and natural spaces.

#### 3.4.1. Evolution of Major Landscape Units

In 2015, the study area was primarily occupied by settlements, covering approximately 53.66% of the total area (3968.30 ha). Agricultural fields and fallows covered 27.22% (≈2013.35 ha), while fields and fallows under palm groves represented 12.18% (900.77 ha).

By 2024, there was a significant expansion of urban areas, with settlements reaching 70.46% of the territory (5210.91 ha), an increase of 1242.61 ha compared to 2015.

#### 3.4.2. Cartographic Analysis of Land Use Changes

Figure 5 and Figure 6 illustrate land use maps for 2015 and 2024, respectively. These maps clearly show:

- Densification of built-up areas, particularly along road networks and within municipal centers.
- Noticeable regression of agricultural and natural formations, especially in peripheral zones.
- Figure 5 displays the dominance of agricultural and fallow lands still prevalent in 2015.
- Figure 6 shows massive urban expansion by 2024, notably in the central and northwestern parts of the study area, accompanied by increased fragmentation of natural spaces.

#### 3.4.3. Quantitative Evolution of Land Use Classes

The bar chart (Figure 7) compares land use areas between 2015 and 2024 and reveals:

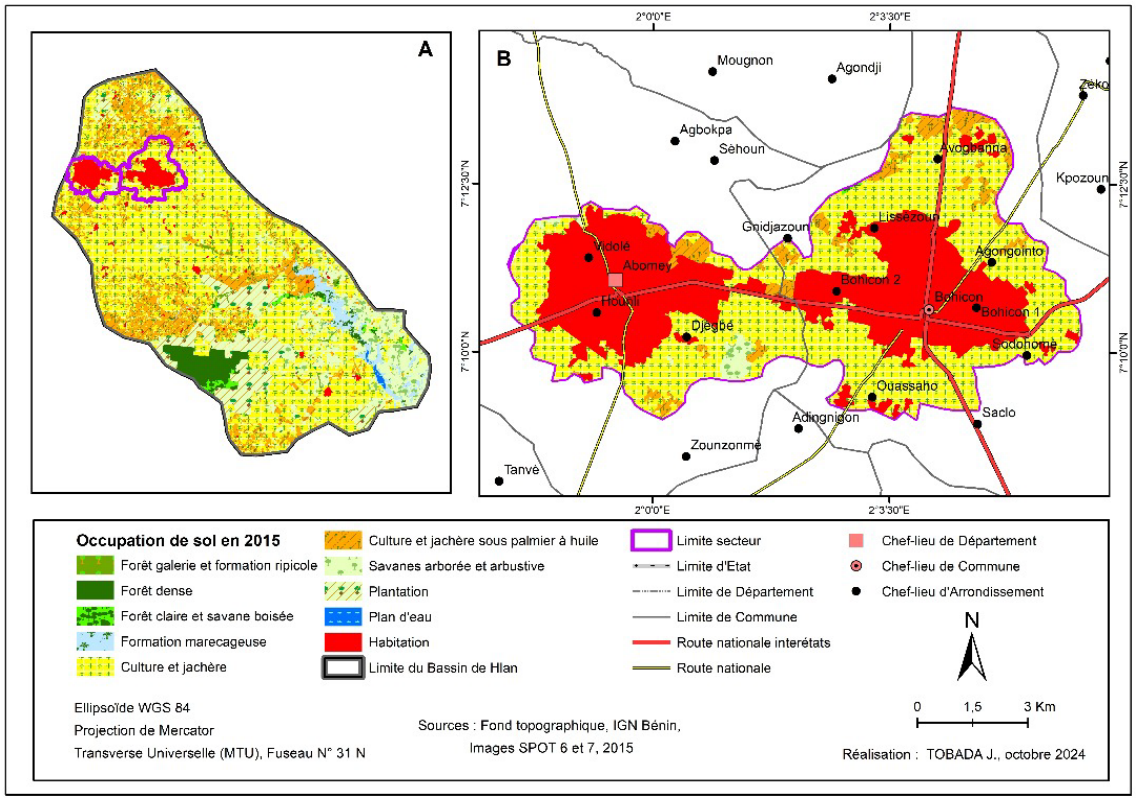


**Figure 5.** Land use mapping of the study area in 2015.

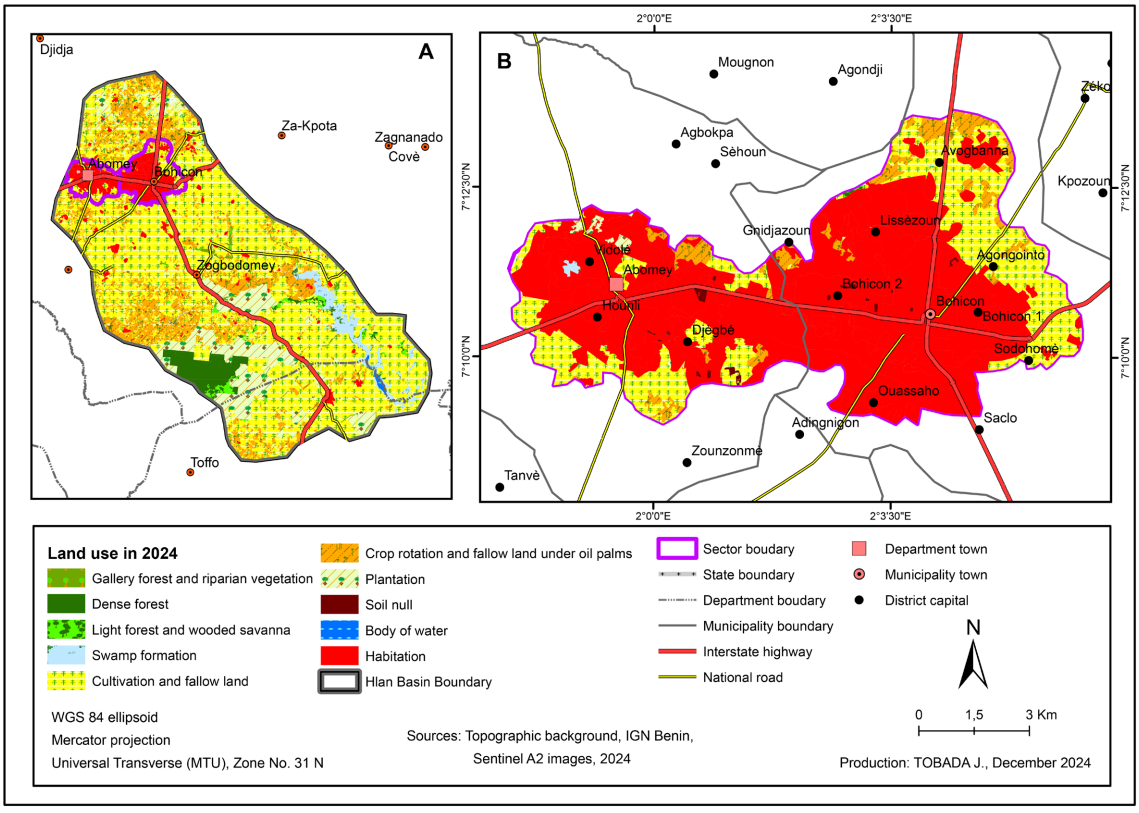


**Figure 6.** Land use mapping of the study area in 2024.

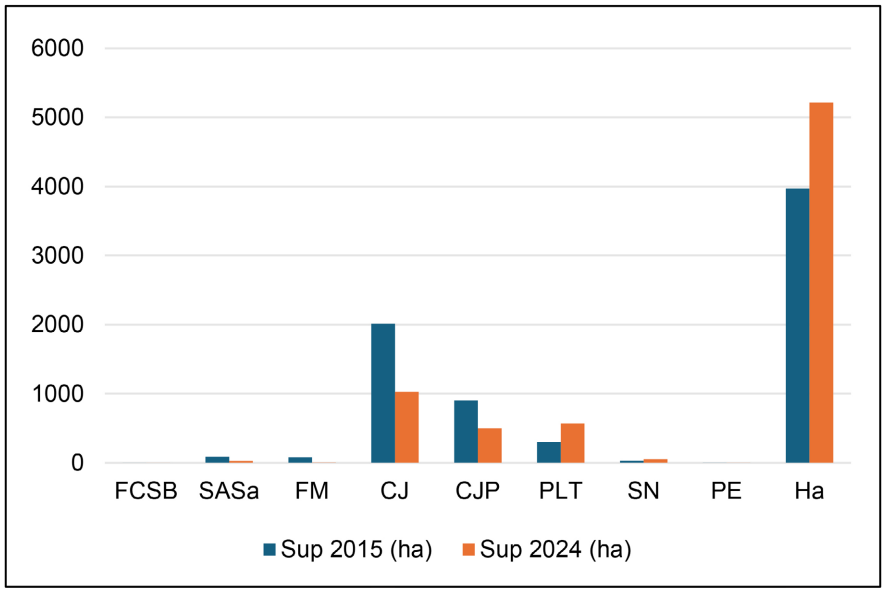


**Figure 7.** Evolution of land use units between 2015 and 2024. FCSB: Open Forest-Wooded Savanna; SASa: Tree-Shrub Savanna; FM: Marshland Formation; CJ: Fields and Fallow; CJP: Fields and Fallow under Palm Groves; PLT: Plantation; SN: Bare Soil; PE: Water Body; Ha: Settlement.

- A sharp decline in fields and fallows (CJ) from 2013.35 ha to 711.75 ha (a loss of 1301.60 ha);
- A reduction in fields and fallows under palm groves (CJP) from 900.77 ha to 368.75 ha;
- A substantial increase in settlements (Ha) from 3968.30 ha to 5210.91 ha;
- Relative stability in other categories such as open forest-wooded savanna (FCSB) and marshland formations (FM), which occupy marginal areas.

The transition matrix (Table 6) details these transformations between 2015 and 2024, highlighting:

- Major conversions to settlements (Ha) from:
  - Fields and fallows (CJ): 1032.72 ha,
  - Fields and fallows under palm groves (CJP): 63.01 ha,
  - Plantations (PLT): 117.88 ha;
- Net losses in most agricultural and natural classes;
- A net gain of 1242.61 ha for the settlement class (+16.80%);
- Low persistence rates in agricultural units:
  - CJ: only 711.75 ha retained out of 2013.35 ha;
  - PLT: only 183 ha retained out of 300.88 ha.

This pattern confirms the increasing anthropogenic pressure, mainly through urban sprawl and the decline of traditional agricultural practices.

The acceleration of urbanization between 2015 and 2024, at the expense of farmland and natural habitats, raises major concerns for urban planning and land management policies. The losses observed in agricultural zones and palm groves could lead to ecological and socio-economic consequences, including:

- Reduced agro-ecological resilience,
- Potential degradation of local ecosystems,
- Increased vulnerability to climate hazards (flooding, erosion),
- Heightened land pressure around urban centers.

Figure 5 and Figure 6 respectively show the land-use mapping of the study area in 2015 and 2024.

Figure 7 then illustrates the quantitative evolution of land-use units between 2015 and 2024. A clear increase in residential areas, exceeding 5200 hectares, can be observed, along with a significant decrease in agricultural land, particularly cultivated fields and fallow land.

To complement this analysis, Table 6 presents the transition matrix of land-use units between 2015 and 2024, expressed in hectares.

Table 6. Land use transition Matrix between 2015 and 2024.

| Land Use Units 2015 | Land Use Units 2024 | | | | | | | | | | |
|---|---|---|---|---|---|---|---|---|---|---|---|
| | **FCSB** | **SASa** | **FM** | **CJ** | **CJP** | **PLT** | **SN** | **PE** | **Ha** | **Total 2015 (ha)** | Loss |
| **FCSB** | 1.00 | 0.00 | 0.00 | 0.00 | 0.00 | 0.00 | 0.00 | 0.00 | 2.00 | **3.00** | 2.00 |
| **SASa** | 0.00 | 25.59 | 0.00 | 25.00 | 5.00 | 3.00 | 7.05 | 0.00 | 25.00 | **90.63** | 65.05 |
| **FM** | 0.00 | 0.00 | 5.91 | 73.59 | 2.00 | 1.00 | 0.00 | 1.00 | 0.50 | **84.00** | 78.09 |
| **CJ** | 0.00 | 0.00 | 0.00 | 711.75 | 126.00 | 128.00 | 14.88 | 0.00 | 1032.72 | **2013.35** | 1301.60 |
| **CJP** | 0.00 | 0.00 | 0.00 | 216.55 | 368.75 | 252.45 | 0.00 | 0.00 | 63.01 | **900.77** | 532.01 |
| **PLT** | 0.00 | 0.00 | 0.00 | 0.00 | 0.00 | 183.00 | 0.00 | 0.00 | 117.88 | **300.88** | 117.88 |
| **SN** | 0.00 | 0.00 | 0.00 | 0.00 | 0.00 | 0.00 | 29.54 | 0.00 | 1.50 | **31.04** | 1.50 |
| **PE** | 0.00 | 0.00 | 0.50 | 0.00 | 0.00 | 0.00 | 0.00 | 3.00 | 0.00 | **3.50** | 0.50 |
| **Ha** | 0.00 | 0.00 | 0.00 | 0.00 | 0.00 | 0.00 | 0.00 | 0.00 | 3968.30 | **3968.30** | 0.00 |
| **Total 2024 (ha)** | **1.00** | **25.59** | **6.41** | **1026.88** | **501.75** | **567.45** | **51.47** | **4.00** | **5210.91** | **7395.46** | **2098.63** |
| **Gain** | 0.00 | 0.00 | 0.50 | 315.13 | 133.00 | 384.45 | 21.93 | 1.00 | 1242.61 | **2098.63** | |

FCSB: Open Forest-Wooded Savanna; SASa: Tree-Shrub Savanna; FM: Marshland Formation; CJ: Fields and Fallow; CJP: Fields and Fallow under Palm Groves; PLT: Plantation; SN: Bare Soil; PE: Water Body; Ha: Settlement.

### 3.5. Evolution of Land Use Units between 2005 and 2015: Conversion Rate, Annual Expansion, and Rate of Change

The comparative analysis between 2005 and 2015 reveals significant transformations in land use units, reflecting a progressive shift from rural landscapes to increasingly anthropized (human-modified) environments. The examination of Conversion Rates (CR), Average Annual Expansion Rates (AER), and Rates of Change (Δs) highlights both regressive and progressive trends among the land-

scape categories.

Table 7 presents the conversion rates (CR), the average annual spatial expansion rates (T), and the evolution speeds (Δs) of landscape units between 2005 and 2015.

Table 7. Conversion rates, average annual expansion rates, and evolution speeds (Progression or Regression) of land use units from 2005 to 2015.

| Land Use Units | Area (ha) 2005 | Area (ha) 2015 | CR (%) | AER (%) | Δs (ha/year) |
|---|---|---|---|---|---|
| FCSB | 22.00 | 3.00 | 86.36 | −8.64 | −1.90 |
| SASa | 151.98 | 90.63 | 41.68 | −4.04 | −6.13 |
| FM | 89.50 | 84.00 | 7.26 | −0.61 | −0.55 |
| CJ | 2518.26 | 2013.35 | 27.61 | −2.01 | −50.49 |
| CJP | 711.77 | 900.77 | 25.29 | 2.66 | 18.90 |
| PLT | 141.25 | 300.88 | 3.54 | 11.30 | 15.96 |
| SN | 12.04 | 31.04 | 0 | 15.78 | 1.90 |
| PE | 4.00 | 3.50 | 25 | −1.25 | −0.05 |
| Ha | 3744.66 | 3968.30 | 0 | 0.60 | 22.36 |

Legend: FCSB: Open forest and wooded savannah, SASa: Shrub and tree savannah, FM: Wetland formation, CJ: Fields and fallow land, CJP: Fields and fallow under palm groves, PLT: Plantation, SN: Bare soil, PE: Water body, Ha: Habitation.

CR (%): Conversion Rate; TS (%): AER: Average Annual Expansion Rate, $\Delta_s$: Rate of Change in ha/year

Key Observations from Table 5:

- Notable Progressions :
  - Habitation (Ha): Moderate yet consistent growth with an AER of 0.6% and an evolution speed of +22.36 ha/year, reflecting steady urbanization.
  - Plantations (PLT): Significant growth (+15.96 ha/year), indicating the intensification of structured agricultural operations.
  - Fields and fallow under palm groves (CJP): Noteworthy increase (+18.90 ha/year), suggesting a growing preference for agroforestry cover.
- Marked Regressions:
  - Fields and fallow (CJ): The sharpest absolute decline: −50.49 ha/year, possibly due to conversion to urban or plantation land.
  - SASa and FCSB: are regressing at −6.13 and −1.90 ha/year respectively, indicating natural habitat loss.
- Stable or Marginal Units:
  - Wetland formations (FM) and water bodies (PE): Minimal variations, implying relative stability or low land pressure on these environments.

### 3.6. Evolution of Land Use Units between 2015 and 2024: Recent Trends in Expansion and Regression

Over the 9-year period (2015-2024), land use dynamics reveal an acceleration of urbanization accompanied by a sharp decline in agricultural and natural spaces. The table below reports conversion rates, average annual expansion, and evolution speeds for the different land use classes.

Table 8 summarizes the conversion rates (CR), average annual expansion rates (T), and evolution speeds (Δs) recorded between 2015 and 2024.

Table 8. Conversion rates, average annual expansion rates, and evolution speeds (Progression or Regression) of land use units from 2015 to 2024.

| Land Use Units | Area (ha) 2015 | Area (ha) 2024 | CR (%) | AER (%) | Δs (ha/year) |
|---|---|---|---|---|---|
| FCSB | 3.00 | 1.00 | 66.67 | −7.41 | −0.22 |
| SASa | 90.63 | 25.59 | 71.77 | −7.97 | −7.23 |
| FM | 84.00 | 6.41 | 92.96 | −10.26 | −8.62 |
| CJ | 2013.35 | 1026.88 | 64.65 | −5.44 | −109.61 |
| CJP | 900.77 | 501.75 | 59.06 | −4.92 | −44.33 |
| PLT | 300.88 | 567.45 | 39.18 | 9.84 | 29.62 |
| SN | 31.04 | 51.47 | 4.83 | 7.31 | 2.27 |
| PE | 3.50 | 4.00 | 14.29 | 1.59 | 0.06 |
| Ha | 3968.30 | 5210.91 | 0 | 3.48 | 138.07 |

Legend: FCSB: Open forest and wooded savannah, SASa: Shrub and tree savannah, FM: Wetland formation, CJ: Fields and fallow land, CJP: Fields and fallow under palm groves, PLT: Plantation, SN: Bare soil, PE: Water body, Ha: Habitation.

CR (%): Conversion Rate; TS (%): AER: Average Annual Expansion Rate, $\Delta_s$: Rate of Change in ha/year

Key Observations from Table 6:

- Accelerated Urbanization:
  - Habitation (Ha): Displays the highest progression speed with +138.07 ha/year. The AER of +3.48% without any class shift (CR = 0%) suggests steady, linear, or outward development.
- Dramatic Decline of Agricultural and Natural Spaces:
  - Fields and fallow (CJ): Lost 986.47 ha in 9 years, *i.e.*, −109.61 ha/year, indicating intensified conversion to urban or plantation land.
  - Wetland formations (FM): experienced the sharpest proportional loss (CR = 92.96%), possibly reflecting land pressure on wetland zones.
  - SASa and CJP: show strong declines at −7.23 ha/year and −44.33 ha/year, respectively.

- Growth in Plantations (PLT):
  - The area under plantations nearly doubled in 9 years, from 300.88 ha to 567.45 ha (+29.62 ha/year), signaling agricultural intensification or controlled reforestation.
- Stability in Marginal Units:
  - Bare soil (SN) and water bodies (PE): Moderate changes, likely due to seasonal dynamics or temporary land use.

Table 9: Evolution of Agricultural Lands and Rates of Change (2005-2024).

Table 9. Comparative summary between the two periods (2005-2015 vs. 2015-2024).

| Indicator | 2005-2015 | 2015-2024 | Trend |
|---|---|---|---|
| Maximum Positive Evolution Speed | Ha (+22.36 ha/year) | Ha (+138.07 ha/year) | ↑ Strong acceleration |
| Maximum Negative Evolution Speed | CJ (−50.49 ha/year) | CJ (−109.61 ha/year) | ↓ Sharp regression |
| PLT Progression | +15.96 ha/year | +29.62 ha/year | ↑ Reinforced expansion |
| CJ + CJP Combined Agricultural Land Loss | −31.59 ha/year | −153.94 ha/year | ↓ Massive decline in farmland areas |

The observed dynamics highlight the urgent need to reflect on:

- Sustainable Urban Planning: To better manage the expansion of built-up areas and avoid uncontrolled sprawl.
- Agricultural Land Management: To safeguard food production capacity in the region.
- Conservation of Wetlands and Natural Areas: As key components of biodiversity and climate resilience.

### 3.7. Intensity of Land Use Changes between 2005 and 2015

The diachronic analysis of land use between 2005 and 2015 allows for an assessment not only of the spatial transformation dynamics of various landscape units but also for identifying zones of stability, gain, and loss. Figure 8 synthetically illustrates these changes as a percentage of the study area, based on three categories: loss, stability, and gain by land use class.

The "Habitation (Ha)" class clearly dominates this observation period. It alone accounts for approximately 54% of the total area of the study sector, of which 51% remained stable and 3% corresponds to gains. Notably, no loss was recorded for this class, highlighting the continuous expansion of urbanization and the consolidation of built-up zones.

In contrast, three landscape units experienced significant losses:

- Fields and fallow land (CJ): with a 10% loss, this class appears to be the most

impacted by land conversion, likely due to increasing urbanization and land pressure.

- Shrub and tree savannah (SASa): this unit experienced a substantial reduction, reflecting ongoing deforestation or a shift toward more anthropized uses.
- Fields and fallow under palm groves (CJP): are also in decline; this class reflects the retreat of specific agroforestry activities (e.g., oil palm cultivation) in favor of other uses (housing, intensive plantations).

On the other hand, certain units, such as plantations (PLT), saw modest gains, suggesting a trend of planned reforestation or targeted commercial agriculture.

These findings indicate an intensification of human activities in the study area, characterized by:

- The consolidation of residential zones (growing urbanization and building density),
- The conversion of agricultural land (especially fields and fallow) into urban or semi-urban uses,
- The progressive decline of natural or semi-natural areas, including tree savannahs and wetland formations.

These spatial changes underscore the need for integrated territorial planning, which should consider land pressure, food security, sustainable natural resource management, and climate resilience challenges.

Figure 8 illustrates the change intensities among the different land-use categories during the period 2005-2015, distinguishing the shares of loss, stability, and gain within each class.

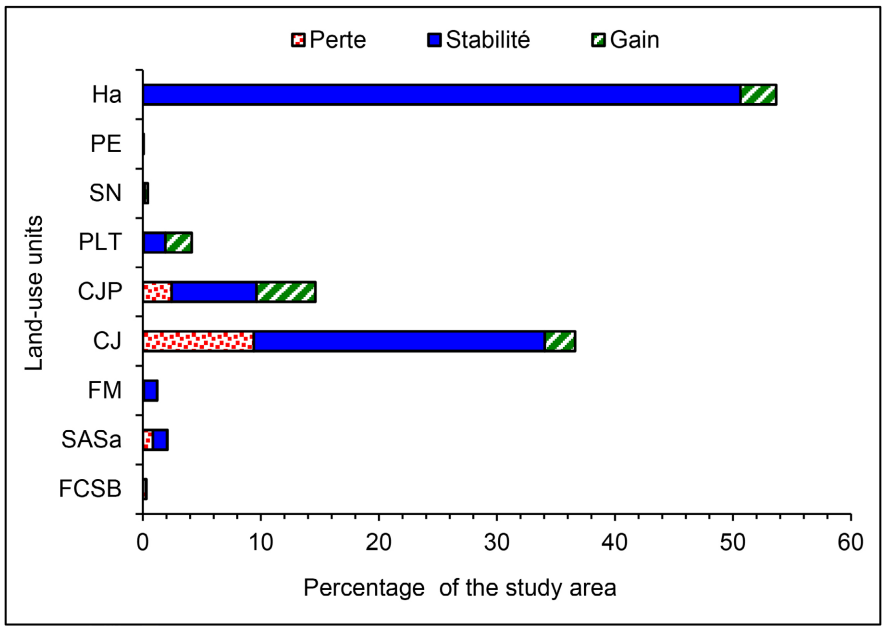


Figure 8. Intensity of land use changes between and within classes (2005-2015). FCSB: Open forest and wooded savannah, SASa: Shrub and tree savannah, FM: Wetland formation, CJ: Fields and fallow land, CJP: Fields and fallow under palm groves, PLT: Plantation, SN: Bare soil, PE: Water body, Ha: Habitation.

### 3.8. Intensity and Rate of Land Use Changes within Categories (2005-2015)

The analysis of the spatio-temporal dynamics of land use provides a key indicator of the anthropogenic pressure exerted on land resources. **Figure 9** illustrates the intensity and speed of land use changes between 2005 and 2015 within each land use category in the study area.

A cross-reading of gain, loss, and intensity values allows for precise characterization of the internal dynamics of each category:

- The "Habitation (Ha)" class recorded only gains, reaching about 15% of land use units, with no losses. This growth reflects accelerated urbanization in the study area. While the level of intensity is high, it remains lower than that of agricultural areas, indicating a gradual but controlled expansion of built-up areas.
- The "Bare Soil (SN)" and "Water Bodies (PE)" categories also recorded only gains, possibly related to the opening of new agricultural fronts or the drying of marshy areas, respectively.
- Conversely, the "Open Forest and wooded savannah (FCSB)" class experienced a complete loss, with no gain, amounting to almost 90% of its initial area. This indicates severe land conversion pressure, particularly toward agricultural or residential uses. This loss is concerning from a natural resource conservation perspective.
- The "Shrub and Tree Savannah (SASa)", "Fields and Fallow (CJ)", and "Fields and Fallow under Palm Groves (CJP)" categories recorded significant net losses, amounting to approximately 65%, 55%, and 45%, respectively, of their initial areas. These categories appear to be the primary contributors to the expansion of residential areas or conversion into plantations or bare lands.
- Plantations (PLT), despite experiencing some losses, exhibited moderate intensity of gains, suggesting a reinforcement of this land use category, potentially driven by reforestation policies or agricultural diversification initiatives.

The blue vertical dashed line in the figure represents the theoretical intensity threshold, beyond which change is considered "rapid or active" (to the right of the line) or "slow or latent" (to the left of the line), according to [16]

- Thus, categories such as FCSB, CJ, CJP, and SASa, located to the right of this line, are undergoing rapid land transformations, indicative of profound structural changes in the rural spatial organization.
- In contrast, classes to the left of this line, such as Water Bodies (PE) or Wetland Formation (FM), indicate low-intensity changes, often sporadic or localized.

These results highlight a strong transformation dynamic in the study area between 2005 and 2015, marked by:

- Massive decline of natural and agricultural areas, especially wooded savannahs and fallow zones.
- Rapid urbanization, with notable acceleration in the "Habitation" category.
- Irreversible losses of natural formations underline the urgency of more bal-

anced and sustainable land use planning.

Figure 9 illustrates the intensity and speed of changes observed within each land-use category during the period 2005-2015.

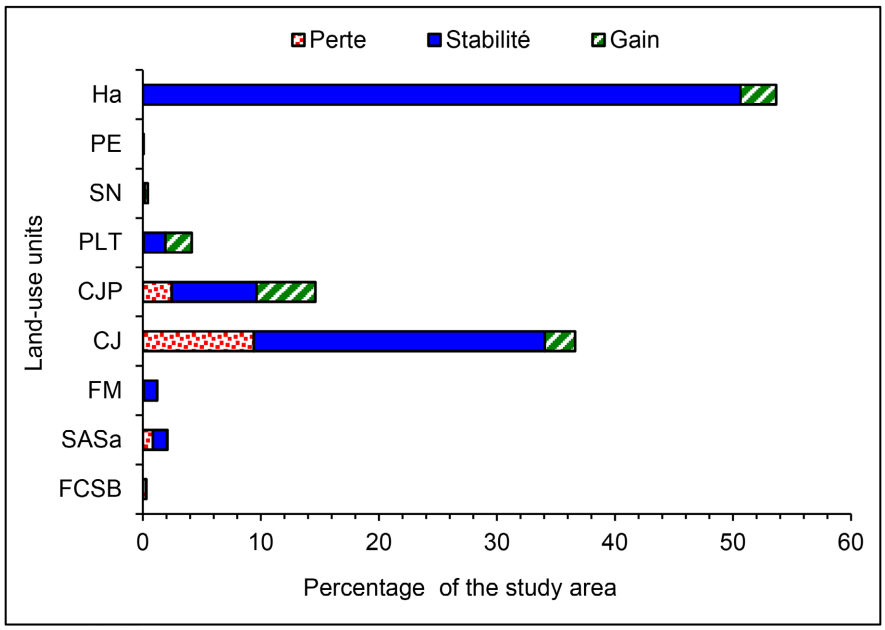


Figure 9. Intensity and speed of changes by land use category in the study area (2005-2015). FCSB: Open forest and wooded savannah, SASa: Shrub and tree savannah, FM: Wetland formation, CJ: Fields and fallow land, CJP: Fields and fallow under palm groves, PLT: Plantation, SN: Bare soil, PE: Water body, Ha: Habitation.

### 3.9. Change Intensities by Time Interval (2015-2024)

The diachronic analysis of land use between 2015 and 2024, presented in Figure 10, highlights the intensity of changes between various landscape categories in the study area.

Reviewing Figure 10 reveals land use dynamics characterized by contrasting changes across classes. These are expressed through both losses and gains, reflecting significant land pressure in some areas, linked to urban expansion and socio-economic shifts.

- The "Habitation (Ha)" class stands out with a positive dynamic:
  - It represents approximately 71% of the study area, of which 54% remains stable and 17% corresponds to new gains.
  - This significant increase reflects rapid urban expansion, likely driven by population growth and infrastructure development.
  - The observed gain exceeds that of the previous period (2005-2015), confirming an acceleration of land artificialization.
- The CJ, CJP, SASa, FM, and PLT classes show notable losses:
  - These categories are the main sources of conversion to residential areas.
  - This indicates a functional reallocation of land, with agricultural and natural areas giving way to urban expansion.

- The FCSB, SN, and PE classes exhibit more marginal behavior:
  - The FCSB class remains barely represented, with no recorded gains, suggesting a near-complete disappearance of this vegetation type.
  - SN and PE show little evolution, with slight gains likely due to natural processes or minor land use changes (e.g., erosion, flooding, sedimentation).

Additional Interpretive Insights:

1) Contextual Factors: Urban expansion must be analyzed through economic, demographic, and political lenses, including spatial planning policies, road infrastructure, and economic activity zones.

2) Overlay with Land Use Maps: Superimposing GIS land cover maps from 2015 and 2024 could help to identify key conversion hotspots.

3) Warning Thresholds: The rapid gain rate in the "Habitation" class raises concerns about biodiversity loss or ecosystem service degradation, justifying the implementation of more sustainable land planning measures.

4) Link with Intensity Analysis (Section 3.8): Comparing the relative intensity of losses and gains per category with temporal intensity helps target high-risk or dynamic areas.

In summary, the 2015-2024 period is marked by intensified urban dynamics, primarily at the expense of agricultural land and shrub savannahs. This finding underscores the need for integrated land management policies to anticipate land use conflicts and preserve the ecosystem balance of the territory.

Figure 10 presents the change intensities among the different land-use categories for the period 2015-2024.

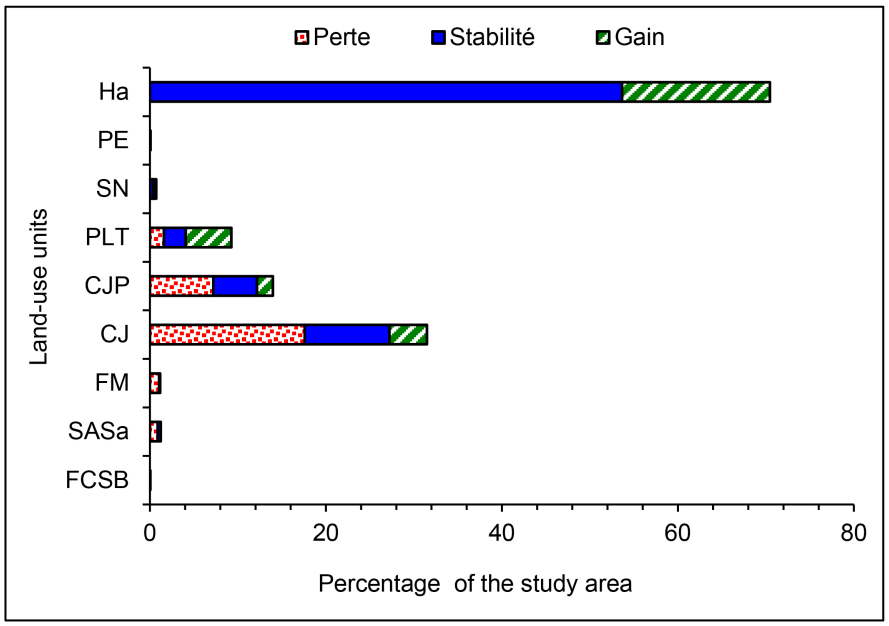


Figure 10. Intensity of changes between and within land use categories (2015-2024). FCSB: Open forest and wooded savannah, SASa: Shrub and tree savannah, FM: Wetland formation, CJ: Fields and fallow land, CJP: Fields and fallow under palm groves, PLT: Plantation, SN: Bare soil, PE: Water body, Ha: Habitation.

### 3.10. Intensity and Speed of Changes within Each Land Use Category (2015-2024)

Figure 11 presents the intensity and speed of changes that occurred within each land use category between 2015 and 2024. It highlights the landscape transformation dynamics over the period, distinguishing between gains, losses, and the relative share of each land use class in relation to the total area of the study sector.

The observation of Figure 11 reveals that all landscape units were affected by change dynamics, with significant variations in terms of intensity (total bar length) and direction (gain or loss):

- The "Habitation" (Ha) class exhibits a particular profile: it recorded no losses during the period, only gains that slightly exceed the dashed blue line, which represents the uniform change threshold. This means that the expansion of built-up areas in the study sector was active and rapid, reflecting increasing anthropogenic pressure due to urbanization and construction expansion.
- The "Water Bodies" (PE) and "Bare Soil" (SN) units also show significant gains, with little to no loss. These gains can be attributed, respectively, to:
  - Hydraulic developments, including expanding natural or artificial water bodies,
  - Soil degradation or deforestation dynamics, leaving exposed surfaces.
- The "Plantation" (PLT) class is the only unit to show both a high gain and a notable loss, suggesting strong spatial instability—with both the creation and removal of plantations, possibly due to shifts in agricultural practices or land use policies.

The following units experienced predominantly or total losses:

- Open Forest and Wooded Savannah (FCSB): recorded only losses, with very high intensity, nearing 90% of its original area. This reflects advanced deforestation or degradation, likely for agricultural or urban conversion.
- Shrub and Tree Savannah (SASa), Wetland Formation (FM), Fields and Fallow (CJ), and Fields and Fallow under Palm Groves (CJP) all show dominant losses, indicating massive land conversion, particularly toward habitation zones or plantations.

These units appear to be the main sources of land conversion for the expansion of urbanized areas and intensive agricultural activities.

The vertical dashed blue line represents the uniform change threshold:

- To the left of this line, changes are considered dormant or slow, indicating relative stability or moderate transformation.
- To the right, changes are active or rapid, pointing to strong instability or major disturbances.

Units such as PLT, SN, CJ, CJP, FM, SASa, and FCSB all fall beyond this threshold, indicating that their transformations were active, rapid, and significant, often driven by anthropogenic pressures, intensive land use shifts, or land reallocation policies.

Between 2015 and 2024, the analysis of change intensity and speed per land use

category reveals a strong territorial transformation dynamic:

- Runaway urbanization is the main driver of these transformations, as evidenced by the net increase in the "Habitation" class.
- Natural and agricultural environments are the most affected by regression, mainly in favor of built-up areas or more intensive farming systems.

These findings underscore the need for integrated and forward-looking territorial management, aiming to reconcile socio-economic development with the preservation of natural resources in the study area.

Figure 11 illustrates the intensity and speed of changes within each landscape unit for the period 2015-2024.

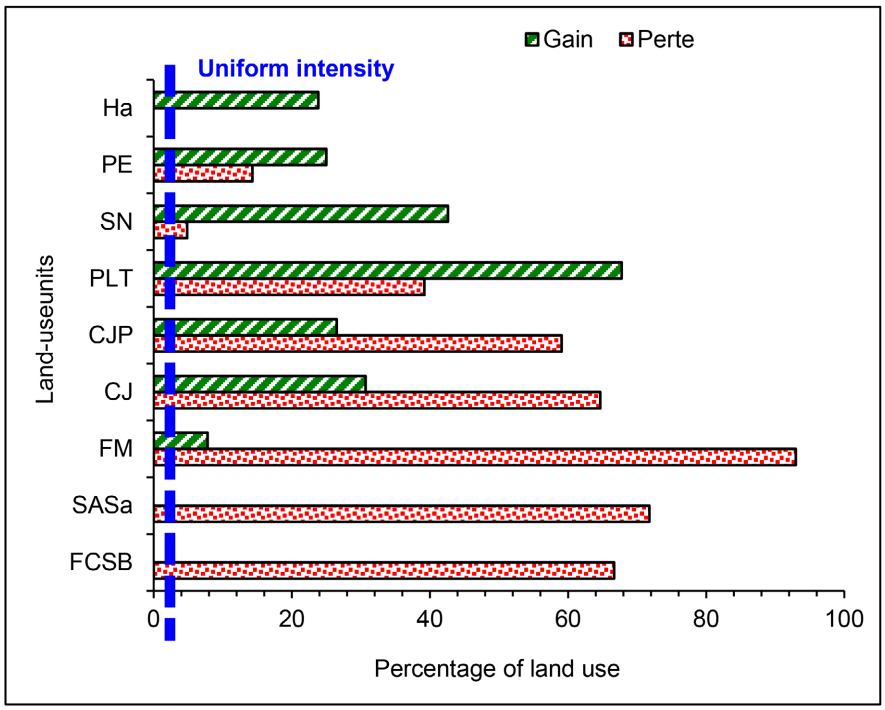


Figure 11. Intensity and speed of changes by land use category in the study area (2015-2024). FCSB: Open forest and wooded savannah, SASa: Shrub and tree savannah, FM: Wetland formation, CJ: Fields and fallow, CJP: Fields and fallow under palm groves, PLT: Plantation, SN: Bare soil, PE: Water body, Ha: Habitation.

### 3.11. Socio-Economic Factors of Urban Expansion

The urban expansion observed over the past two decades is not solely driven by demographic pressure, but also by a set of closely related socio-economic and institutional factors. The development of road infrastructure and urban facilities has increased the attractiveness of peripheral areas, promoting land speculation and the rapid conversion of agricultural lands into built-up areas. At the same time, internal migration, motivated by the search for employment and better living conditions, has intensified the demand for housing and services. The growing monetization of the land market, combined with often insufficient regulation, has further amplified this dynamic by facilitating private appropriation of land. Moreover,

the diversification of economic activities—such as commerce, crafts, transport, and services—has reinforced population concentration along key exchange corridors. These combined processes reflect rapid and often unplanned urbanization, highlighting the need for more integrated territorial governance to balance urban development, social equity, and environmental resource preservation.

### 3.12. Impacts on the Water Cycle

The water cycle is a fundamental natural process regulating life on Earth. It is based on dynamic exchanges between various hydrological components (atmosphere, soil, aquifers, water bodies, etc.) through processes such as infiltration, evapotranspiration, runoff, and percolation. However, accelerated urbanization and the increasing imperviousness of surfaces disrupt this natural cycle by deeply altering water flows within ecosystems.

When natural surfaces are replaced by impermeable materials (concrete, asphalt, rooftops, paving), the soil's infiltration capacity drastically decreases. This transformation leads to:

- A reduction in groundwater recharge, as rainwater is prevented from infiltrating into the soil [17];
- A significant increase in surface runoff, causing faster and larger water flows toward natural outlets [18];
- A direct transport of pollutants (heavy metals, hydrocarbons, nutrients, etc.) to aquatic environments, due to the lack of natural soil filtration [19].

These alterations not only increase flood risks, but also reduce groundwater availability and degrade aquatic ecosystems.

In summary, soil sealing, compounded by the effects of climate change, disrupts the natural balance of the water cycle among infiltration, evaporation, and runoff. This dual pressure increases the vulnerability of territories to flooding, reduces groundwater recharge, and exacerbates the pollution of aquatic environments, thereby compromising environmental sustainability and urban resilience.

#### Imperviousness Rate

The imperviousness rate (I) represents the proportion of impervious surfaces in relation to the total area of a given territory [20]:

$$I = 100 \times \frac{\sum (C_i \times S_i)}{S_t}$$

where:

- $C_i$ is the imperviousness coefficient associated with each surface type $S_i$,
- $S_t$ is the total area of the study zone.

Figure 12 illustrates the evolution of both land use and the imperviousness rate in Bohicon from 2005 to 2025. The results indicate a pronounced urbanization dynamic, with a gradual reduction of agricultural and fallow land and open forest and wooded savannah, in favor of residential areas:

- In 2005, imperviousness represented approximately 15% of the territory.
- In 2015, it approached 20%, with relative stability in other land use classes.
- By 2025, it reaches nearly 30%, reflecting a significant expansion of built-up areas.

This trend illustrates a growing artificialization of land, driven by rapid urbanization and a lack of sustainable stormwater management mechanisms. Natural surfaces are losing their buffering capacity, leading to:

- More frequent and severe floods,
- Alteration of hydrogeological balances,
- Increased degradation of receiving water quality.

Figure 13 shows the evolution of imperviousness in Abomey over the same period. The trend is similar to that observed in Bohicon, albeit slightly less intense:

- In 2005, the imperviousness rate was about 15%.
- It increased to 19% in 2015.
- In 2025, it reaches approximately 25%, with a visible expansion of residential zones at the expense of shrubby and tree savannahs and croplands.

This growth, although more moderate than in Bohicon, still reflects ongoing urbanization. The associated risks are similar, but could be less severe if urban resilience policies are implemented in time.

Table 10. Evolution of imperviousness and associated land-use changes and risks in Bohicon and Abomey (2005-2025).

Table 10. Comparison between bohicon and abomey.

| Parameter | Bohicon (2005 → 2025) | Abomey (2005 → 2025) |
|---|---|---|
| Evolution of Imperviousness Rate | 15% → 30% | 15% → 25% |
| Most Reduced Classes | Crops, Forests | Crops, Savannahs |
| Strongest Increasing Class | Habitation | Habitation |
| Major Risks | Flooding, Pollution | Flooding |

The land use transformations in Bohicon and Abomey reflect an intense urbanization process with tangible hydrological impacts. The increase in impervious surfaces directly affects the water cycle by reducing infiltration, increasing runoff, and amplifying environmental risks.

Therefore, sustainable urban planning that integrates green infrastructure (e.g., infiltration trenches, vegetated swales, green roofs) is essential to partially restore the soil's natural functions. In addition, detailed hydrodynamic studies are needed to assess the resilience capacity of these environments in the face of climate change and urban expansion.

Figure 12 and Figure 13 show the evolution of the imperviousness rate in the cities of Abomey and Bohicon.

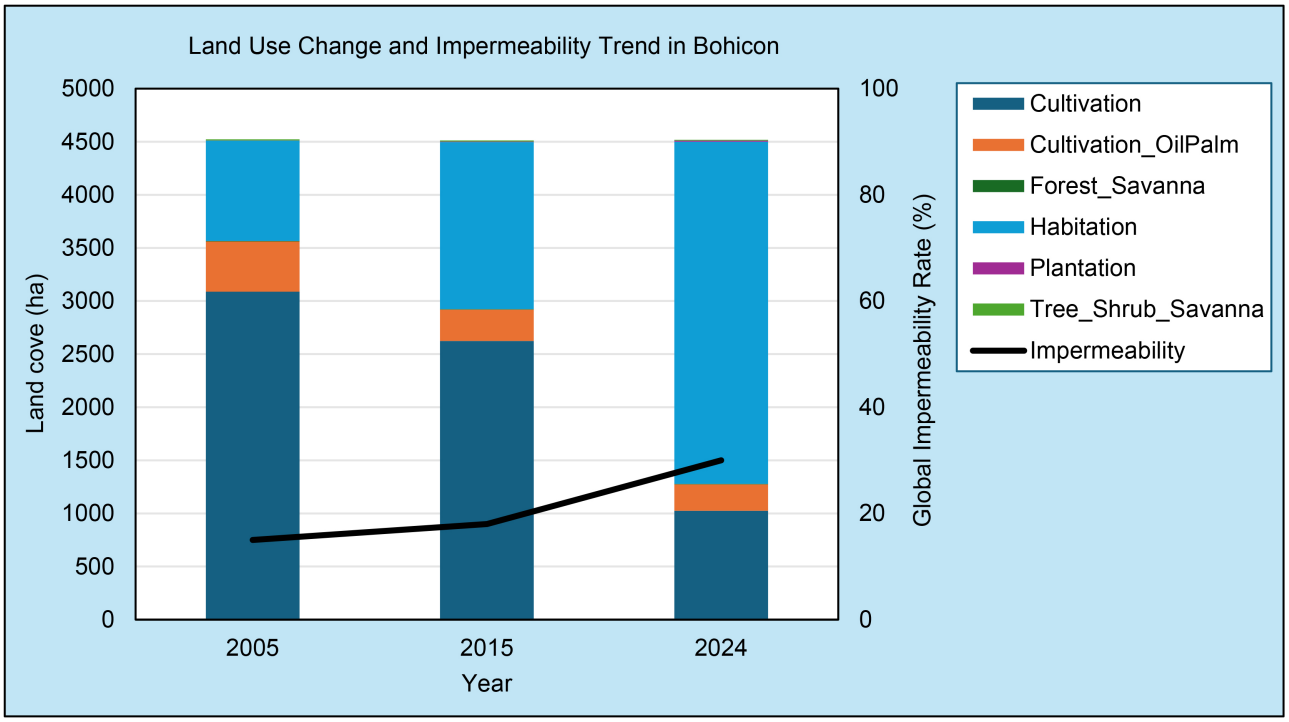


**Figure 12.** Evolution of imperviousness in Bohicon.

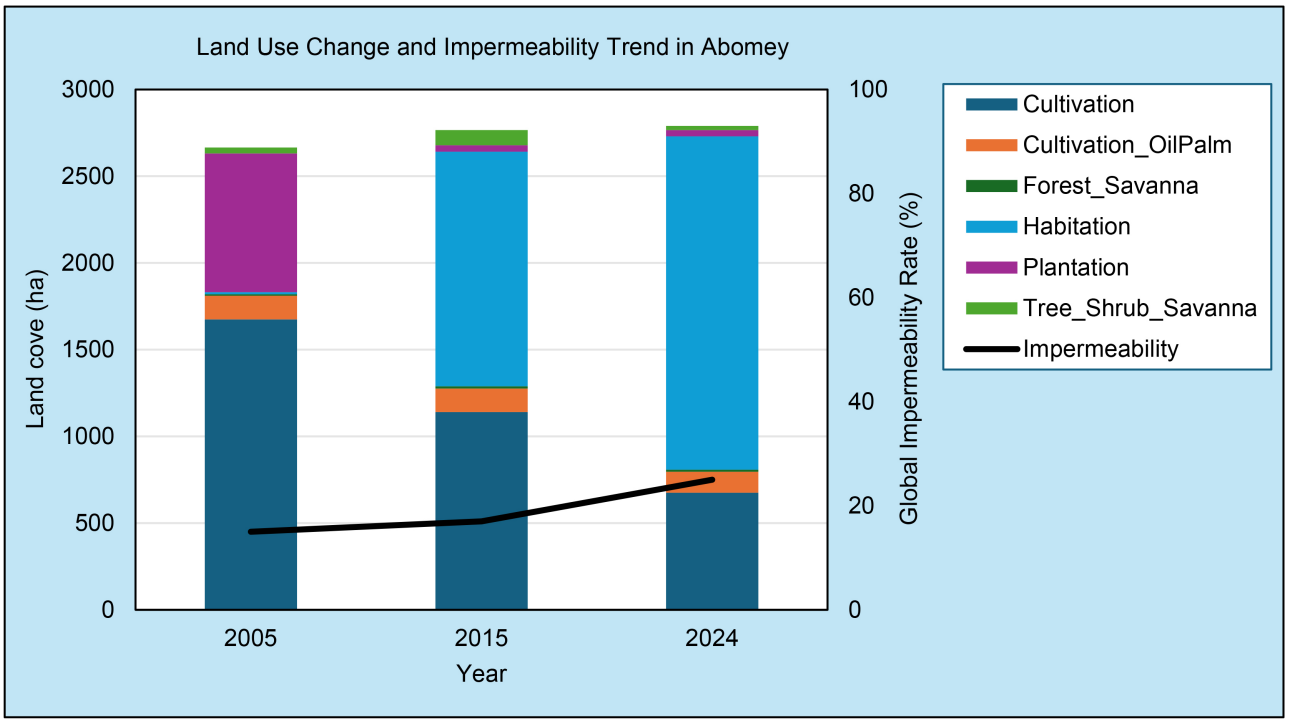


**Figure 13.** Evolution of imperviousness in Abomey.

### 3.13. Impacts on Natural Water Flow

Urban expansion in the cities of Abomey and Bohicon has taken place without considering the natural rainwater flow corridors. The superimposition of spatial

data on built infrastructure with the natural water flow directions (Figure 14 and Figure 15) highlights the chaotic occupation of areas that are sensitive to hydrological drainage.

Figure 14 shows that in the municipality of Abomey, many built structures (roads, subdivisions, buildings) intersect or block the natural drainage paths, which are indicated in the background. The accumulation of infrastructure on these corridors hinders water circulation, reducing infiltration capacity and increasing runoff velocity.

Similarly, Figure 15, which relates to Bohicon, illustrates an even more critical situation: the natural drainage axes are largely covered or fragmented by the urban fabric. The phenomenon is exacerbated in densely built-up areas, particularly in the city center and expanding peri-urban zones.

Main Consequences of Hydrological Corridor Occupation

1) Increased Flood Risk: When runoff zones are sealed (roads, roofs, concrete slabs), rainwater can no longer infiltrate the soil. It is thus redirected over the surface toward low-lying areas, leading to a rapid concentration of water volumes during heavy rainfall events.

This results in localized overflows, prolonged water stagnation, and even flash floods. These dynamics align with the observations of [21], who demonstrated that infrastructure in unmanaged runoff zones exacerbates the hydrological vulnerability of urban areas.

2) Accelerated Soil Erosion: Diverting water from its natural path artificially creates concentration zones of hydrological flow, often over bare or sloped surfaces. The resulting erosion manifests as gullies, rills, and progressive degradation of unpaved roads or building foundations. This erosion, coupled with the absence of a suitable drainage network, weakens existing urban infrastructure and may lead to landslides or superficial ground movement over time [22].

Table 11. Observed water flow patterns, built-up areas, and potential vulnerability in Abomey and Bohicon.

Table 11. Technical Interpretation of Figure 14 and Figure 15.

| Observed Element | Figure 14 (Abomey) | Figure 15 (Bohicon) |
|---|---|---|
| **Water flow direction** | Convergence toward the south and east, hindered by roads and subdivisions | Multiple radial axes, heavily interrupted by urban densification |
| **Built-up areas conflicting with the flow** | Historic center, north-south axes | City center, west, and southeast extensions |
| **Potential vulnerability** | Medium to high, especially in the northeast | High in all directions except northeast, which remains relatively free |

Recommendations for Improved Hydrological Resilience

1) Flood-prone Area Mapping: Based on natural hydrology and fine topography, to regularize urban development.

2) Urban Planning Integration: Develop a land-use plan that respects natural water flow, especially in steep slope areas or near temporary streambeds.

3) Implementation of Sustainable Drainage Systems (SUDS): Including retention basins, vegetated swales, green roofs, to control runoff intensity.

4) Awareness-Raising Among Local Stakeholders: Educate municipal authorities, residents, and developers about the risks of chaotic occupation of water corridors.

The spatial analysis of natural water flow in Abomey and Bohicon reveals a clear disconnect between urban development and natural hydrological dynamics. This inconsistency heightens the risks of flooding and soil erosion, threatening the long-term sustainability of urban infrastructure.

An integrated land management approach—combining urban planning, ecology, and hydrology—is essential for protecting these cities against the growing challenges of climate change and urban sprawl.

Figure 14 and Figure 15 illustrate the direction of natural flows in the cities of Abomey and Bohicon, highlighting areas of blockage and runoff concentration due to uncontrolled urbanization.

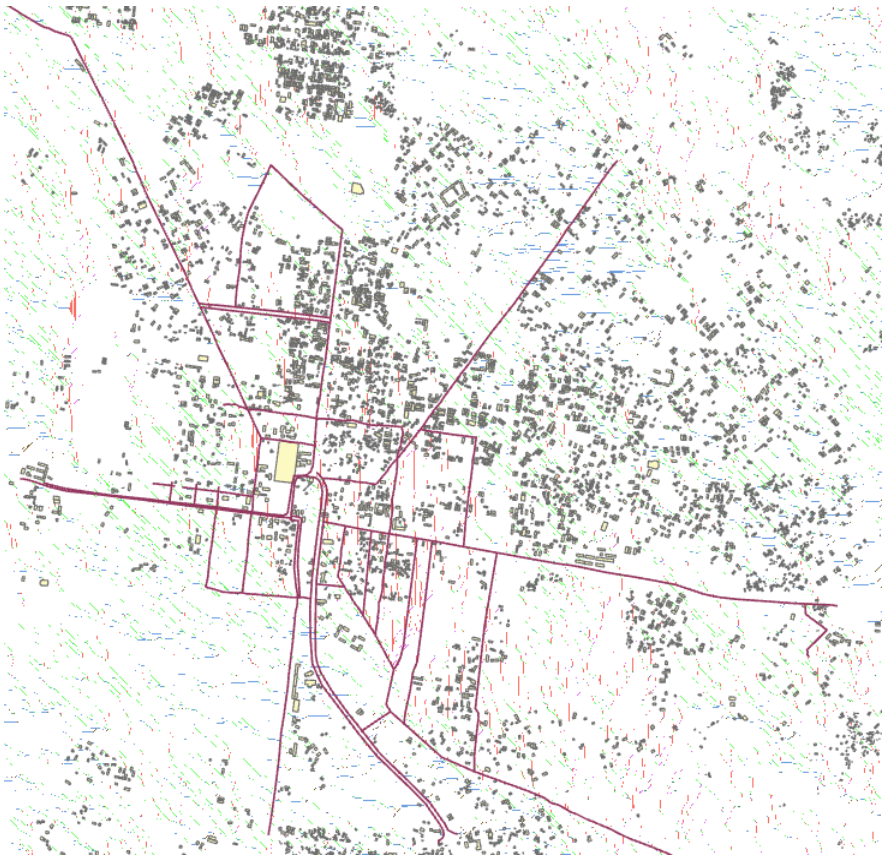

**Figure 14.** Natural water flow directions in Abomey.

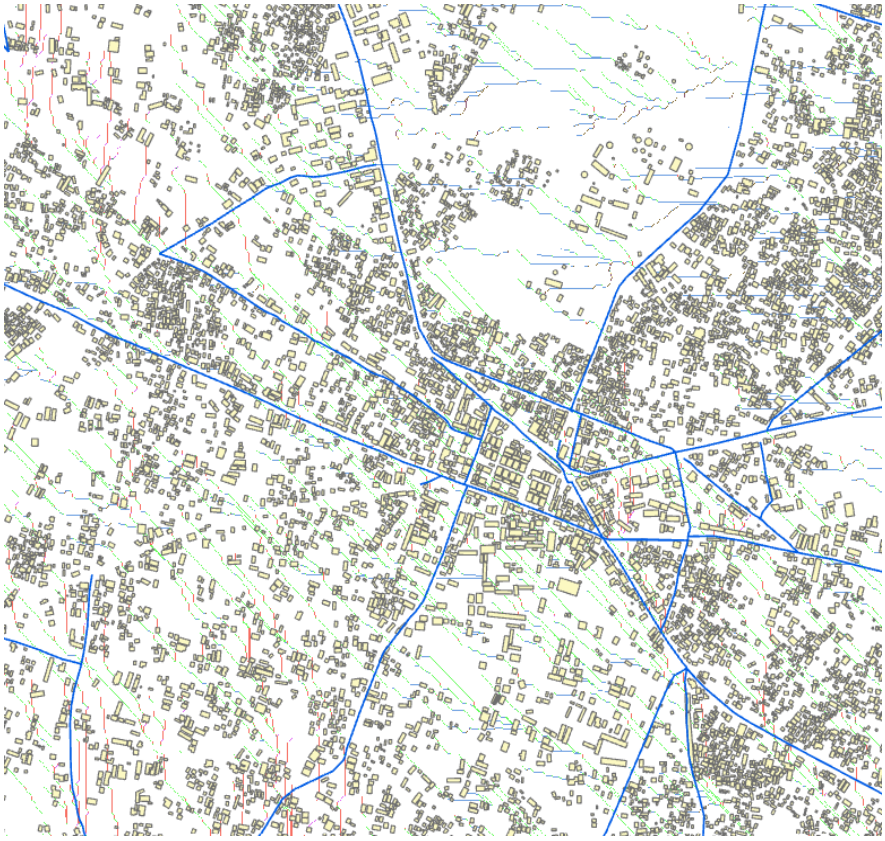

Figure 15. Natural water flow directions in Bohicon.

## 4. Study Limitations

Despite the methodological rigor adopted, this study presents certain limitations that should be highlighted. On the one hand, the spatial resolution of satellite images may introduce uncertainties in the fine detection of land-use changes, particularly in highly heterogeneous areas or those with complex landscape mosaics. On the other hand, the analysis relies mainly on cartographic and statistical approaches, without integrating direct hydrological modeling to quantitatively assess the impact of soil sealing on peak flows or flood return periods. Finally, some seasonal or interannual variations in climatic conditions were not fully incorporated into the analysis, which could influence the observed dynamics. Nevertheless, these limitations do not undermine the relevance of the results but suggest avenues for future research combining spatial analysis with integrated hydrological modeling.

## 5. Conclusions

The analysis of the spatio-temporal dynamics of land use between 2005, 2015, and 2024 highlights a major structural transformation of the landscapes in the cities of Abomey and Bohicon, characterized by rapid, extensive, and often unplanned urbanization. The results derived from thematic maps and transition matrices reveal a continuous expansion of built-up areas, increasing from 50.64% in 2005 to

70.46% in 2024, representing a gain of more than 1240 hectares in less than two decades. This growth has occurred primarily at the expense of croplands and fallows, fallows under oil-palm plantations, and natural vegetation formations, whose areas have significantly decreased. The reduction of vegetation cover, combined with increasing soil sealing, has profoundly altered the hydrological functioning of the territory and increased the basin's vulnerability to runoff and flooding.

This dynamic reflects a rapid and spatially uneven landscape transformation, driven by demographic pressure, urban sprawl, and weak territorial planning mechanisms. The uncontrolled expansion of residential areas and the progressive occupation of low-lying or flood-prone zones directly contribute to the degradation of the natural drainage network, the concentration of surface flows, and the recurrence of floods observed in several neighborhoods of Abomey and Bohicon.

From an institutional and policy perspective, these results call for a reorientation of urban planning and stormwater management strategies within a framework of urban resilience. It is essential for municipal authorities to adopt an integrated territorial management approach based on:

- Sustainable and participatory urban planning, taking into account flood-prone areas and observed land-use dynamics.
- Preservation and restoration of vegetated areas, including fallows, plantations, and wetlands, which provide essential infiltration and hydrological regulation functions.
- Modernization and regular maintenance of drainage infrastructure, favoring nature-based solutions such as swales, retention basins, and permeable gutters;
- Awareness-raising and empowerment of local populations regarding sustainable land management and control of urban expansion;
- Integration of remote sensing, GIS, and hydrodynamic modeling tools (HEC-RAS, SWMM) into local planning and risk management policies.

Thus, the 2005-2024 period illustrates an accelerated process of environmental artificialization, requiring coordinated and forward-looking policy interventions to preserve ecological balance, reduce flood vulnerability, and guide urban development toward a more resilient, inclusive, and sustainable trajectory.

## Conflicts of Interest

The authors declare no conflicts of interest regarding the publication of this paper.

## References

[1] Benziada, H. (2019) Urbanisation et vulnérabilité aux risques d'inondation en milieu urbain: Cas de la ville d'Alger. *European Science Journal*, **15**, 294-312.

[2] Redjem, A. (2020) Urban Sprawl and Flood Risk: A Spatial Analysis in the City of Batna, Algeria. *European Journal of Geography*, **11**, 136-150.

[3] Azioune, M. (2018) Urbanisation et risques environnementaux en milieu urbain: Cas

de la ville de Constantine. *Les Cahiers d'Afrique de l'Ouest*, **6**, 15-27.

[4] Barattucci, C. (2010) Vulnérabilité urbaine face aux inondations: Enjeux et outils d'évaluation spatiale. L'Harmattan.

[5] Institut Géographique National (1955) Carte topographique et administrative du Dahomey. Institut Géographique National (IGN)—Annexe de Dakar.

[6] Kioko, M. (2010) Land Use Cover and Environmental Changes in a Semiarid Rangeland, Southern Kenya. *Journal of Geography and Regional Planning*, **3**, 322-332.

[7] Toko, I. (2014) Modélisation des dynamiques d'occupation du sol dans la commune de Bohicon. Université d'Abomey-Calavi.

[8] ESRI (2018) ArcGIS Desktop 10.6 Help: Intersect (Analysis), Version 10.6. Redlands, Environmental Systems Research Institute.

[9] Pontius, K. (2004) Useful Techniques of Validation for Spatially Explicit Land-Change Models. *Ecological Modelling*, **179**, 445-461. https://doi.org/10.1016/j.ecolmodel.2004.05.010

[10] Sébastien Kouta, M. (2020) De la dynamique de la flore dans le bassin cotonnier. These de Doctorat Spécialité, Université d'Abomey-Calavi (Bénin).

[11] Kpoha, J.N., Akokponhoue, H.B., Orekan, V., *et al.* (2023) Contribution de la télédétection et d'un SIG à la cartographie des unités de l'occupation du sol et ses changements face au problème d'inondation sur le plateau d'Allada au Benin. *International Journal of Innovation and Scientific Research*, **65**, 164-177.

[12] Arouna, O. (2012) Cartographie et modélisation prédictive des changements spatio-temporels de la végétation dans la Commune de Djidja au Bénin: Implications pour l'aménagement du territoire. Thèse de Doctorat, Université d'Abomey-Calavi, Bénin.

[13] Antoni, J.-P. and Thévenot, J. (2008) Modéliser les dynamiques d'urbanisation pour accompagner la planification territoriale. *Association de Sémiologie et de Recherche sur la Dialectologie et la Linguistique Françaises*, Rimouski, 25-27 August 2008, 1-12.

[14] Aldwaik, G. (2012) Intensity Analysis to Unify Measurements of Size and Stationarity of Land Changes. *Annals of the Association of American Geographers*, **102**, 839-858.

[15] Aldwaik, G. (2012) Intensity Analysis to Unify Measurements of Size and Stationarity of Land Changes by Interval, Category, and Transition. *Landscape and Urban Planning*, **106**, 103-114. https://doi.org/10.1016/j.landurbplan.2012.02.010

[16] Pontius Jr., M. (2004) Detecting Important Categorical Land Changes while Accounting for Persistence. *Agriculture, Ecosystems & Environment*, **101**, 251-268. https://doi.org/10.1016/j.agee.2003.09.008

[17] Haase, H. (2007) Urban Land Use Changes and Their Ecological Consequences. *Landscape and Urban Planning*, **81**, 1-13.

[18] Natale, F. (2007) Modelling of Flood Propagation in Urban Areas. *Hydrological Processes*, **21**, 3264-3279.

[19] Hope, B. (2004) Impact of Land Use on Water Quality in Urban Ecosystems. *Environmental Pollution*, 124, 353-363.

[20] Díez-Herrero, A., Mateos, R.M., Vázquez-Tarrío, D., López-Marcos, A. and Brao-González, F.J. (2024) One Catastrophic Flood Every Millennium: Synchronicity of Extreme Floods and Global Warm Periods in the Multi-Archive Record of the Roman Theatre of Guadix (Granada, SE Spain). *Global and Planetary Change*, **233**, Article 104363. https://doi.org/10.1016/j.gloplacha.2024.104363

[21] Pauleit, S., Ennos, R. and Golding, Y. (2005) Modeling the Environmental Impacts of Urban Land Cover Change—A Study in Merseyside, UK. *Landscape and Urban Plan-*

*ning*, **71**, 295-310. https://doi.org/10.1016/S0169-2046(04)00083-0

[22] Brun, S.H. (2017) Urban Infrastructure Degradation and Slope Instability in Expanding Cities. *Natural Hazards*, **81**, 945-962.